



Long-term ecological assessment of intracranial electrophysiology synchronized to behavioral markers in obsessive-compulsive disorder

Nicole R. Provenza^{ID 1,2}, Sameer A. Sheth³, Evan M. Dastin-van Rijn^{ID 1}, Raissa K. Mathura³, Yaohan Ding⁴, Gregory S. Vogt⁵, Michelle Avendano-Ortega⁵, Nithya Ramakrishnan⁵, Noam Peled^{ID 6,7}, Luiz Fernando Fracassi Gelin⁸, David Xing¹, Laszlo A. Jeni⁹, Itir Onal Ertugrul¹⁰, Adriel Barrios-Anderson¹¹, Evan Matteson¹, Andrew D. Wiese^{5,12}, Junqian Xu^{ID 5,13}, Ashwin Viswanathan³, Matthew T. Harrison¹⁴, Kelly R. Bijanki^{3,5}, Eric A. Storch⁵, Jeffrey F. Cohn^{ID 15}, Wayne K. Goodman^{5,18} and David A. Borton^{ID 1,16,17,18}

Detection of neural signatures related to pathological behavioral states could enable adaptive deep brain stimulation (DBS), a potential strategy for improving efficacy of DBS for neurological and psychiatric disorders. This approach requires identifying neural biomarkers of relevant behavioral states, a task best performed in ecologically valid environments. Here, in human participants with obsessive-compulsive disorder (OCD) implanted with recording-capable DBS devices, we synchronized chronic ventral striatum local field potentials with relevant, disease-specific behaviors. We captured over 1,000 h of local field potentials in the clinic and at home during unstructured activity, as well as during DBS and exposure therapy. The wide range of symptom severity over which the data were captured allowed us to identify candidate neural biomarkers of OCD symptom intensity. This work demonstrates the feasibility and utility of capturing chronic intracranial electrophysiology during daily symptom fluctuations to enable neural biomarker identification, a prerequisite for future development of adaptive DBS for OCD and other psychiatric disorders.

OCD has a lifetime prevalence of 2–3% and is a leading cause of disability worldwide¹. Pharmacological and cognitive behavioral therapy are the mainstays of treatment but fail to provide sustained benefit in 25–40% of individuals¹. Approximately 10% of individuals fail to achieve benefit from any intervention². For severe, treatment-refractory cases of OCD, neurosurgical procedures have been used with varying degrees of success for half a century¹. Modern neurosurgical approaches include both stereotactic lesion procedures and DBS, with roughly similar response rates¹. Over half of patients with treatment-resistant OCD are responders to DBS targeted to the ventral capsule/ventral striatum (VC/VS) region³. Beyond marked improvement in OCD symptoms, VC/VS DBS has been found to improve anxiety, depression, mood and quality of life even in patients who are nonresponders to DBS treatment^{4,5}. To date, the number of patients who have received DBS for OCD worldwide is in the hundreds⁶. Many more individuals may qualify for DBS but do not receive or pursue this treatment course due to various barriers (for example, awareness, access and cost) or treatment preferences.

One of the main advantages of DBS over other neurosurgical approaches (for example, stereotactic lesion procedures) is its adjustability. Stimulation parameters can be varied and optimized to maximize beneficial effects and minimize adverse effects. This programmability is an important reason why DBS is more common than lesion procedures in the surgical treatment of movement disorders such as Parkinson's disease and essential tremor⁷. However, adjusting DBS parameters for OCD management differs notably from that for movement disorders. Whereas stimulation effects (both beneficial and adverse) typically occur over seconds to minutes in movement disorders, the delay is much longer in psychiatric disorders. Reductions in OCD symptoms usually manifest weeks to months after initiation of DBS stimulation⁴, producing a mismatch in time constants between an adjustment and its effect. Further complicating management is the natural temporal variation of symptom severity within individuals⁸. These factors together impose great barriers to the clinician's attempt to align stimulation parameter adjustments with the moving target of symptom fluctuations.

¹Brown University School of Engineering, Providence, RI, USA. ²Charles Stark Draper Laboratory, Cambridge, MA, USA. ³Department of Neurosurgery, Baylor College of Medicine, Houston, TX, USA. ⁴Intelligent Systems Program, University of Pittsburgh, Pittsburgh, PA, USA. ⁵Menninger Department of Psychiatry and Behavioral Sciences, Baylor College of Medicine, Houston, TX, USA. ⁶MGH/HST Martinos Center for Biomedical Imaging, Charlestown, MA, USA. ⁷Harvard Medical School, Cambridge, MA, USA. ⁸Center for Computation and Visualization, Brown University, Providence, RI, USA. ⁹Robotics Institute, Carnegie Mellon University, Pittsburgh, PA, USA. ¹⁰Department of Cognitive Science and Artificial Intelligence, Tilburg University, Tilburg, the Netherlands. ¹¹The Warren Alpert Medical School of Brown University, Providence, RI, USA. ¹²Department of Psychology, University of Missouri-Kansas City, Kansas City, MO, USA. ¹³Department of Radiology, Baylor College of Medicine, Houston, TX, USA. ¹⁴Division of Applied Mathematics, Brown University, Providence, RI, USA. ¹⁵Department of Psychology, University of Pittsburgh, Pittsburgh, PA, USA. ¹⁶Carney Institute for Brain Science, Brown University, Providence, RI, USA. ¹⁷Center for Neurorestoration and Neurotechnology, Rehabilitation R&D Service, Department of Veterans Affairs, Providence, RI, USA. ¹⁸These authors jointly supervised this work: Wayne K. Goodman, David A. Borton. e-mail: david_borton@brown.edu

An emerging strategy for surmounting these challenges is the development of adaptive, responsive, closed-loop DBS^{9–11}. Current DBS therapy often operates in an open loop, wherein parameter adjustments are made ad hoc during periodic clinic visits weeks or months apart. Continuous stimulation at fixed parameters between clinical visits may inadequately address the temporal dynamics of neurological or psychiatric illnesses, in which symptoms vary over minutes to days. Additionally, stimulation can cause undesirable side effects if applied when not needed³. A responsive, closed-loop, adaptive DBS (aDBS) system may improve efficacy by titrating stimulation parameters in response to real-time neural signatures (that is, biomarkers) related to symptoms and side effects.

The last few years have witnessed a rapid expansion in the application of aDBS strategies and technology for use in movement disorders^{12–15}. Successful demonstrations of aDBS, notably in Parkinson’s disease, have emphasized the need for reliable, symptom-specific behavioral readouts that map to electrophysiological biomarkers¹⁶. For example, beta-band power in the subthalamic nucleus is a well-recognized candidate biomarker for certain symptoms in Parkinson’s disease¹⁷. Unlike in movement disorders, however, there is currently no objective behavioral readout (for example, diminished tremor in Parkinson’s disease) in psychiatric disorders that clinicians can gauge in real time to optimize DBS parameters. Instead, in psychiatric disorders, clinicians rely on standardized subjective symptom scales to guide therapy delivery such as DBS parameter adjustments¹⁸.

These two factors—the temporal mismatch between symptom evolution and typical DBS adjustment schedule, and the lack of an objective biomarker of psychiatric symptom severity—highlight the monumental challenges facing psychiatric neurosurgery. At the same time, they also underscore the great opportunity for aDBS¹⁹. Our work seeks to address these challenges by recording neural activity during natural, day-to-day OCD symptom fluctuations to begin understanding these critical neural-behavioral relationships.

Recently available devices have provided the technology necessary for both streaming brain electrophysiological data and performing closed-loop control of stimulation parameters^{20,21}. Wireless streaming of neural data outside the clinic is key to robust biomarker discovery, as it enables the collection of neural data under ecological conditions and over extended periods of time, capturing the dynamics of symptom state and neural correlates of behavior. Others have demonstrated the feasibility and utility of such platforms for recording at home from participants with epilepsy and Parkinson’s disease^{22–24}.

Here, we present a longitudinal collection of electrophysiological, behavioral and clinical evaluations from five participants with severe, refractory OCD treated with DBS as part of an ongoing clinical trial toward developing aDBS for OCD (NCT04281134 and NCT03457675). In participants with a psychiatric disorder, we demonstrate the utility of not only in-clinic but also at-home collection of time-synchronized, multimodal brain and behavioral data, which vastly increases both the quantity and ecological validity of the recorded data. We used computer-vision machine learning techniques on video recordings of the participant’s face to assess moment-to-moment changes in emotional state, time-locked with intracranial and extracranial neural recordings. We have captured over 1,000 h of intracranial recordings during behavioral tasks and daily activities at home, labeled with ecological momentary assessment of symptom state. Additionally, we conducted intracranial VC/VS recordings during provocations of symptoms with concomitant administration of two treatment modalities: DBS and exposure and response prevention (ERP) teletherapy. Lastly, based on a series of pilot recordings collected during natural OCD exposures and ERP teletherapy, we demonstrate the ability to measure VC/VS spectral power during natural OCD symptom provocations at home. Continued opportunities for long-term, naturalistic

intracranial electrophysiological recordings will propel biomarker discovery for OCD and other psychiatric disorders.

Results

Study design. Five participants (P1, P2, P3, P4 and P5) with long-standing refractory OCD underwent surgery for bilateral placement of DBS leads capable of applying stimulation and bipolar sensing of neural activity. Longitudinal intracranial electrophysiological data were collected in the clinic and at home from three study participants (P3, P4 and P5). Electrophysiological recordings were time-locked to behavior and DBS parameter changes in the clinic, and momentary self-report of OCD symptoms, ERP therapy and behavioral tasks at home (Fig. 1).

Information on participant demographics, stimulation contact, bipolar sensing contact pair, stimulation parameters and responder status, defined by a 35% reduction in Yale-Brown Obsessive Compulsive Scale II (Y-BOCS II) score²⁵, is included in Supplementary Table 1. All five participants were responders to DBS therapy (Supplementary Table 1).

DBS electrodes target the ventral capsule/ventral striatum and bed nucleus of the stria terminalis. Leads were placed in either the VS or the bed nucleus of the stria terminalis (BNST) and superjacent white matter based on intraoperative findings during awake testing. Due to individual specificity, therapeutic response was evaluated on both sides of the anterior commissure (AC) to determine the optimal stimulation target within the broader VC/VS region. In participants P1 and P2, stimulation targets were the left and right BNST (Extended Data Fig. 1). In participant P3, stimulation targets were the left and right VS (Extended Data Fig. 1). In participant P4, stimulation targets were the left VS and right BNST (Fig. 2a–d), and in participant P5, the stimulation targets were the left and right BNST (Extended Data Fig. 1).

Participants P1 and P2 were implanted with the Activa PC+S system, and participants P3, P4 and P5 were implanted with the Summit RC+S system. The Medtronic Summit RC+S rechargeability and wireless data transmission enables streaming of time-domain intracranial electrophysiological recordings both in the clinic and at home, which is not possible with the Activa PC+S system, or any other therapeutic DBS platform. In addition, the Medtronic Summit RC+S system offers improved artifact rejection and sensing performance compared to the Activa PC+S system²⁰. Therefore, herein we focus on data gathered from the three participants implanted with the Summit RC+S.

Longitudinal recordings show stability over time. To gauge the quality of the longitudinal recordings over time, impedance of sensing and stimulation electrodes for P3, P4 and P5 was measured during the study (Extended Data Fig. 2). Variation in impedance between the sensing contacts and implanted neural stimulator (INS) hermetic enclosure (that is, case) ranged from 705Ω to $1,303\Omega$ for P3 over 101 d, 933Ω to $1,910\Omega$ for P4 over 405 d and 703Ω to $1,468\Omega$ for P5 over 181 d (all measured at 100 Hz), reflecting long-term stability in the device-tissue interface.

Increase in positive affect captured during DBS programming. During clinical DBS programming sessions, intracranial electrophysiological signals were synchronized to behavioral, physiological and electrophysiological measures to develop biomarkers for closed-loop control of stimulation. We used video recordings of the participant’s face (Fig. 3a) to estimate positive affect (Fig. 3b) and head velocity (Fig. 3c) as objective measures of the anxiolytic and anxiogenic responses to changes in DBS parameters (Methods). Positive affect was estimated using automatic facial affect recognition (AFAR), which provides an objective, well-validated approach to quantify subtle changes in affective responses (that is,



Fig. 1 | Streaming of intracranial electrophysiological data in the clinic and at home. Top left, data collection in the clinic during DBS programming. Streaming intracranial electrophysiology (LFPs) from the Summit RC + S, along with EEG, ECG, BVP and video. Top right, Data collection at home during symptom provocation (for example, compulsive hand washing). Streaming LFPs and capturing self-reported intensity of OCD symptoms on a phone. Bottom, data collection at home during sleep. Streaming LFPs and capturing self-reported start and stop times of sleep on an iPhone.

mirth, smiles and brow furrows) intraoperatively and thereafter²⁶. Additionally, we recorded external electrophysiological signals, including blood volume pulse (BVP), electrocardiogram (ECG; Fig. 3d) and 64-channel electroencephalography (EEG; Fig. 3e) and synchronized these signals to changes in DBS parameters (for example, DBS amplitude; Fig. 3f), VS and/or BNST local field potential (LFP) recordings (Fig. 3g), and Summit RC + S acceleration (Fig. 3h). As a demonstrative example, we observed an increase in positive affect of participant P5 in response to an increase in stimulation amplitude, highlighted by a captured smile corresponding to the peak in positive affect estimation during a period of DBS programming where amplitude was incrementally increased from zero to 4.5 mA in steps of 0.5 mA. During and following an increase in DBS amplitude, participant P5 also described positive feelings, including a physical sensation in which ‘internally trembling’ was no longer present (Supplementary Video 1). Clinical experience and limited empirical data suggest that this subjective, positive response to increase

in DBS amplitude is a typical response that may be predictive of treatment outcome²⁷.

Intracranial local field potentials during natural symptom variation at home. We then sought to collect intracranial electrophysiological data in more ecologically valid conditions by using the Summit RC + S system to wirelessly stream intracranial electrophysiology during routine activities in the participants’ homes. At home, participants used a custom tablet application (frontend, <https://github.com/openmind-consortium/App-OCD-PatientFrontend/>; backend, <https://github.com/openmind-consortium/App-OCD-PatientBackend/>) to initiate intracranial VC/VS and/or BNST recordings and perform psychophysiological tasks (<https://github.com/brown-ccv/honeycomb/>)²⁸. Participants reported their OCD symptom intensity and sleep start/stop times using the StriveStudy OCD mobile application (Rune Labs; iPhone XR). Self-reported measures were time synchronized

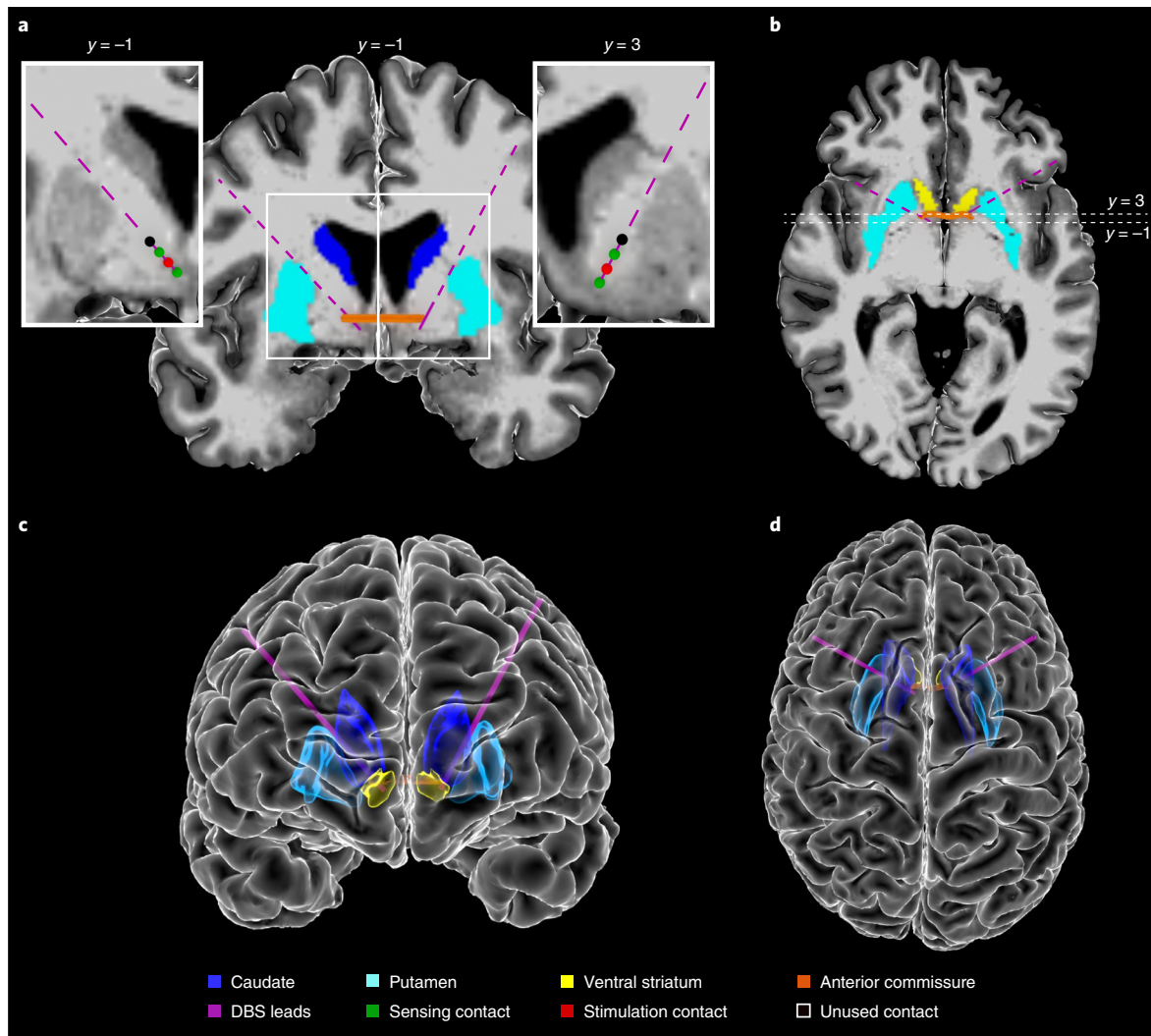


Fig. 2 | Anatomical localization of DBS lead placement. **a,b**, Coronal (**a**) and axial (**b**) T1-weighted (T1w) magnetic resonance imaging (MRI) in radiographic convention from participant P4 overlaid with reconstructed DBS lead trajectories. Colored regions indicate the AC, caudate, putamen and VS. The MRI slice shown is immediately posterior (**a**; coronal) or inferior (**b**; axial) to the most ventral contact. Enlarged coronal slices (corresponding to white box outlines in **a**) showing DBS contact locations in each hemisphere are shown on either side of the full coronal slice. Green spheres indicate sensing contacts, red spheres indicate stimulating contacts, and black spheres indicate contacts that were used for neither stimulation nor sensing. Here, the tip of the left lead was targeted to the VS, and the tip of the right lead was targeted to the BNST. Enlarged slices shown are immediately posterior to the most ventral contact in each hemisphere. Anteroposterior slice location (*y*) is referenced to the posterior border of the AC, which is defined as *y* = 0. **c,d**, Front (**c**) and top-down (**d**) view of the reconstructed cortical surface, subcortical structures, DBS leads and AC, shown in radiographic convention.

with electrophysiological recordings via Network Time Protocol (Methods). Self-reported intensity of OCD symptoms and Y-BOCS II scores were collected after DBS was turned on for participants P3, P4 and P5 (Fig. 4a). Y-BOCS II was administered during clinical visits, while self-reported symptom intensity was captured on a daily basis, or more frequently, by each participant through the StriveStudy OCD application. Interestingly, self-reported values for P4 showed that even after a significant reduction in Y-BOCS II score at week 27, a high day-to-day variability in symptom intensity (range, 0–8; s.d., 0.43–2.81) remained between clinical visits. Such variation in self-reports may have many sources but motivates the need for an adaptive control system to titrate neuromodulation therapy to symptom dynamics. Participants P3 and P5 exhibited less variability in symptom intensity, with ranges of 6–8 and 4–9, respectively (P3 s.d., 0–0.5; P5 s.d., 0–1.34).

While untreated OCD has a stable course²⁹, symptom intensity and severity is recognized to fluctuate within shorter time intervals

(for example, hours and days)³⁰. Therefore, it was critical to develop a technology platform capable of collecting large datasets over long time periods. In total, to date, participants P3, P4 and P5 have collected 52, 813 and 207 h of Summit RC+S intracranial electrophysiology and accelerometry data at home, respectively (Fig. 4b), totaling over 1,000 h. Each intracranial neural recording was matched to self-reported OCD symptom intensity ratings, behavioral tasks and ERP teletherapy sessions. Behavioral tasks relevant to functional domains implicated in OCD were self-administered once per week at home during participant-controlled neural recording sessions (Methods). We synchronized task behavior with neural recordings and calculated the number of hours of neural data collected during behavioral tasks for each participant (P3, 15 h; P4, 37 h; P5, 8 h). Participant P4 completed a multiday ‘sprint recording’ during which over 24 h of data were collected, including Apple Watch heart rate and acceleration, RC + S acceleration and LFPs and self-reported intensity of OCD symptoms (Fig. 4c,d).

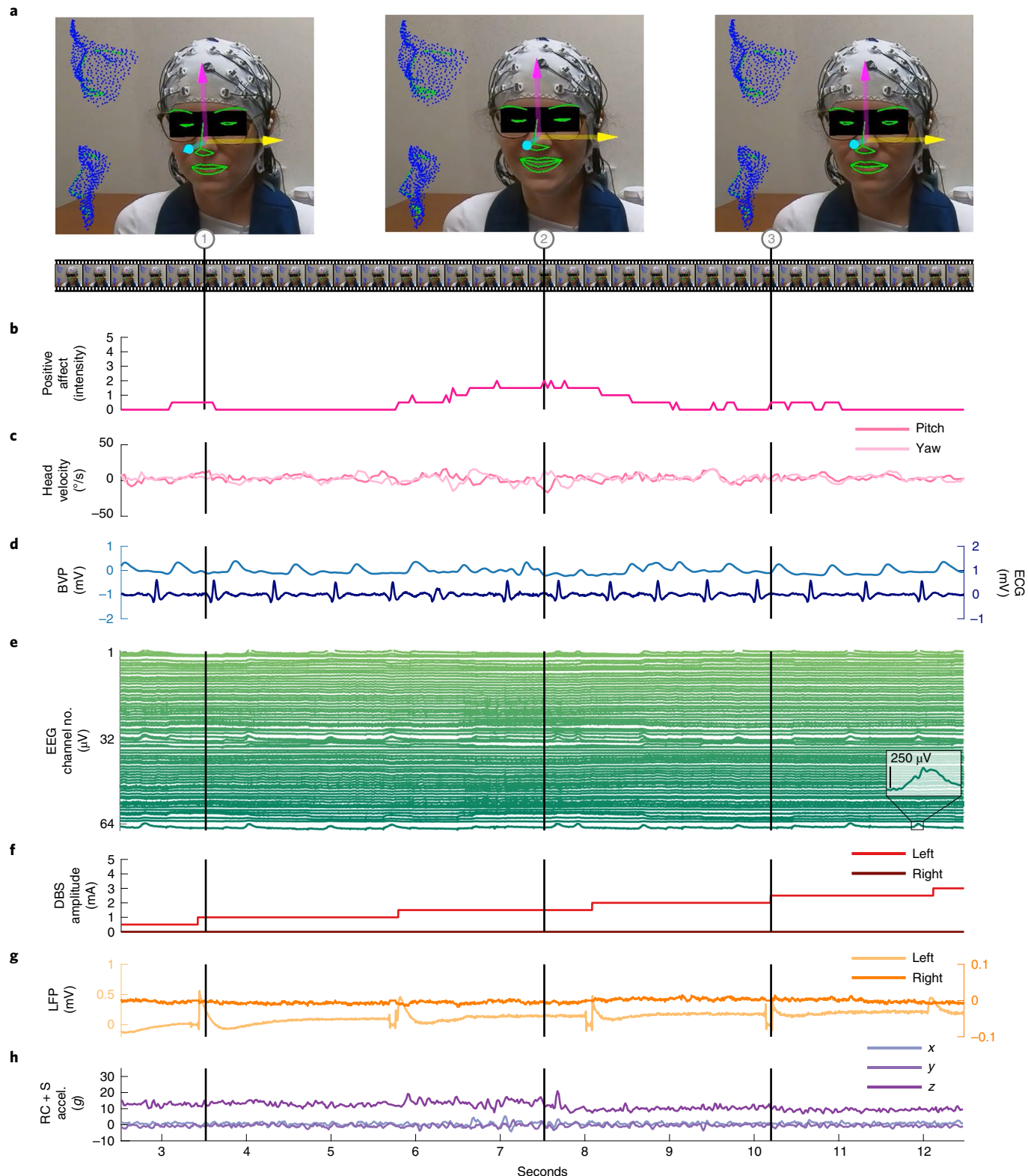


Fig. 3 | Intracranial ventral striatum local field potentials synchronized with continuous affect estimation during DBS programming for OCD. Data correspond to the initial DBS programming session for participant P5. **a**, Video recording of the face (Used with permission) was used to do automatic three-dimensional (3D) face tracking. Arrows indicate the tracked head pose with three degrees of freedom. The contours of tracked key facial parts are highlighted in green. The three video frames (1, 2 and 3) shown correspond to the time points indicated by the vertical lines. **b**, Estimation of positive affect on a scale of zero to five based on facial action units 6 and 12. **c**, Estimation of head velocity in terms of yaw and pitch in units of degrees of displacement per second. **d**, BVP and ECG. **e**, 64-channel EEG. **f**, DBS amplitude. **g**, Bilateral (left and right hemisphere) VS LFP recordings. **h**, RC + S acceleration (xyz).

Intracranial local field potentials during planned and natural exposures. Capturing intracranial electrophysiology during ERP teletherapy sessions is particularly relevant toward the goal of identifying a neural biomarker of OCD-related distress. The capability to record intracranial electrophysiology that is time-locked to naturalistic exposures to OCD triggers at home is a critical technological advancement that may enable discovery of ecologically valid biomarkers in psychiatry. During ERP teletherapy sessions, we recorded a video of the participant and clinician during OCD trigger exposures (Fig. 5b). Throughout the ERP sessions, participants were asked to rate their subjective units of distress (SUDs) in response to each exposure at various time intervals (Fig. 5c). SUD ratings across all ERP sessions ranged from 4 to -6 for P3, and 3 to -10 for P4 and 1 to 8 for P5 (Extended Data Fig. 3). We synchronized ERP teletherapy video and SUD ratings to LFPs, and Summit RC + S and Apple Watch acceleration and heart rate for participants P3 (Extended Data Fig. 4), P4 (Fig. 5d and Supplementary Video 2) and P5 (Extended Data Fig. 5).

To demonstrate the utility of at-home data collection toward biomarker identification, we sought to gain insight on how spectral power changes with OCD symptoms. We analyzed neural data collected from P4 during a 3-d continuous recording session. A total of 41 OCD symptom intensity ratings ranging from zero to eight were reported during neural recordings over the 3-d span ($\mu = 4.49 \pm 2.57$; Fig. 6a). We chose this particular recording for analysis and demonstration due to the occurrence of natural exposures that led to relatively high variability and range in self-reported OCD symptom intensity. Average normalized spectral band power in predefined frequency bands of interest (delta, 0–4 Hz; theta, 4–8 Hz; alpha, 8–15 Hz; beta, 15–30 Hz; gamma, 30–55 Hz) was computed for LFP data collected 1 min before and after each self-report (Methods). Delta-band power in particular showed a strong negative correlation with OCD symptom intensity in both the left (Fig. 6b; $R = -0.593$) and right (Fig. 6b; $R = -0.557$) VC/VS. While the data suggest that the correlation between delta-band power and symptom intensity may be statistically significant, further investigation will be required to determine the consistency of this relationship across individuals. All other frequency bands of interest (theta, 4–8 Hz; alpha, 8–15 Hz; beta, 15–30 Hz; gamma, 30–55 Hz) exhibit relatively weaker correlations with OCD symptom intensity (absolute $R < 0.343$).

We repeated the same spectral analysis for one ERP session during concurrent intracranial neural recordings for participants P3, P4 and P5, and found variable correlations between spectral power in between frequency bands and SUD ratings (Extended Data Figs. 6–8). These analyses reveal the utility of chronic intracranial LFP data for identifying relationships between neural activity and behavior (in this case, psychiatric symptoms). In one participant (P4), the relationship we observed between delta-band spectral power and self-reported symptoms was preserved across natural exposures (Fig. 6b) and planned exposures during ERP teletherapy (Extended Data Fig. 7). Future work will determine the degree of consistency of these brain-behavior relationships across patients and their potential as a biomarker for aDBS applications.

Discussion

Wireless streaming of intracranial electrophysiological data in both the clinic and naturalistic environments provides a rich data source for biomarker discovery. An electrophysiological biomarker of

symptom state would enable aDBS for OCD and other psychiatric disorders, which may provide a better approach for treating fluctuations in symptom intensity¹¹. Here, we acquired electrophysiological data with behavioral readouts over both short and long timescales. In the clinic, we examined changes in affect (AFAR) during DBS parameter changes over short timescales (seconds to minutes). At home during participant-controlled recordings, we captured behavioral changes (self-reported OCD symptoms) over longer timescales (days to weeks to months) in natural settings, collected continuous data during natural and planned exposures, and developed methods to synchronize behavioral metrics to intracranial electrophysiology. Further, we demonstrated the utility of at-home data collection for biomarker identification by observing correlations between spectral power and self-reported OCD symptom intensity.

Only with recent advances in device technology is it now possible to collect intracranial electrophysiological time-synchronized data with rich behavioral markers in ecologically valid environments from patients with neurological or psychiatric disorders. For example, Gilron et al. have described a platform for simultaneous intracranial electrophysiology and wearable accelerometer sensors in natural settings with individuals who have Parkinson's disease²⁴. As an example, using another recording-capable device, Topalovic et al. described a platform for simultaneous EEG, wearable sensors, VR and intracranial electrophysiology, all contained in a small backpack. Their work demonstrates a major advance in collecting both a neurally and behaviorally rich dataset in freely moving humans²³. Here, we demonstrated the application of recent technological advances to record intracranial electrophysiology data time-locked with behavioral events in patients with a psychiatric disorder in natural settings and at chronic timescales.

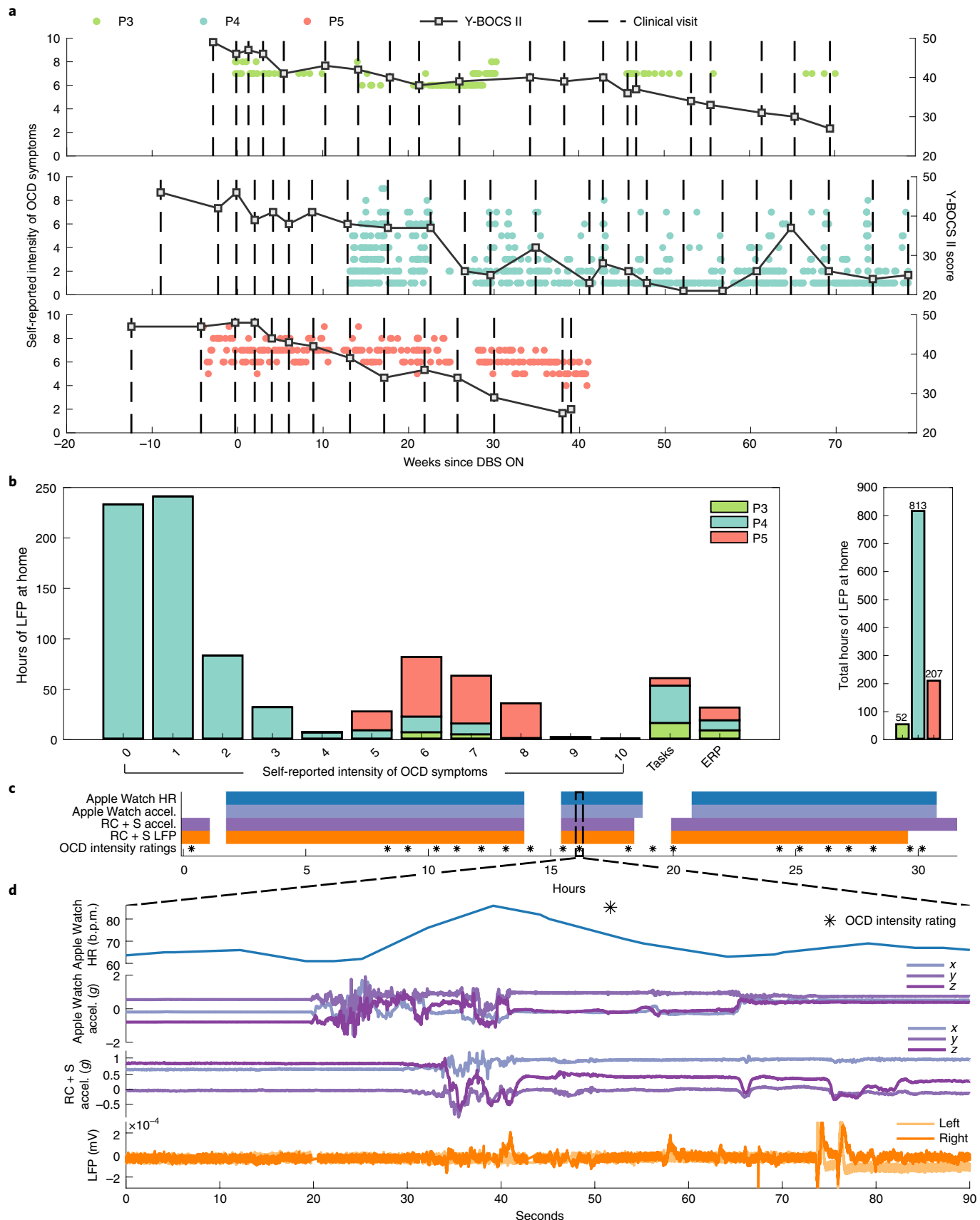
Conducting ecological recordings with a psychiatric population poses several key challenges that are important to address in future work. First, compliance of study participants is variable, and self-reported psychological data are often inaccurate³¹. Intracranial electrophysiology collected over a wide, dynamic range of symptom severity is needed to build a classifier, and such a range may not always be available. We have observed that participants are more likely to comply with daily recordings when they are feeling well, and more likely to avoid engaging in recordings when OCD symptoms are exacerbated. Such reporting bias inherently limits the ecological nature of these recordings. Until we have the ability to trigger home recordings without engagement from the participant, the timing of naturalistic recordings will always be subject to the participant's motivation, anxiety and mood. Additionally, a lack of overlap in OCD subtypes and timescales of symptom fluctuation among our small cohort of participants will likely require personalization of biomarkers and adaptive stimulation paradigms.

In future experiments, we expect to need to implement more extensive mood and symptom logging at home, in addition to tracking more objective measures of patient state such as activity level (for example, number of steps and distance traveled from home) and engagement in social activities (for example, smartphone use). The utility of self-reported assessments is limited as they rely on patient insight into their own psychological state, which is variable³¹. Additionally, we observed that some participants may become superstitious about acknowledging that OCD symptoms have subsided and tend to report a stagnant trend in symptom intensity even after experiencing clinical benefit. More quantitative and objective

Fig. 4 | At-home symptom monitoring synchronized with ecologically valid intracranial electrophysiology. **a**, Y-BOCS II scores, and self-reported intensity of OCD symptoms over weeks since DBS ON in P3, P4 and P5. Square black scatter points indicate Y-BOCS II scores. Circular scatter points indicate one symptom intensity rating from 0–10, and vertical dashed lines denote DBS programming clinical visits. **b**, Number of hours of LFP data collected at home for P3, P4 and P5 corresponding to self-reported intensity of OCD symptoms ratings, behavioral tasks, ERP sessions and in total. **c**, Example data availability plot for an at-home sprint recording over 32 h, completed by participant P4. Shaded portions indicate data availability for Apple Watch heart rate (HR), Apple Watch acceleration, RC + S acceleration, RC + S LFP and OCD intensity ratings. **d**, 90 s of example data corresponding to the dashed-line callout in **c**.

measures have proven useful for tracking Parkinson's disease severity at home and could have equal utility for tracking severity of psychiatric symptoms³².

Additional studies should examine the behavioral task data we collected both in the clinic and at home to assess function in cognitive control, impulsivity and evidence accumulation. Candidate



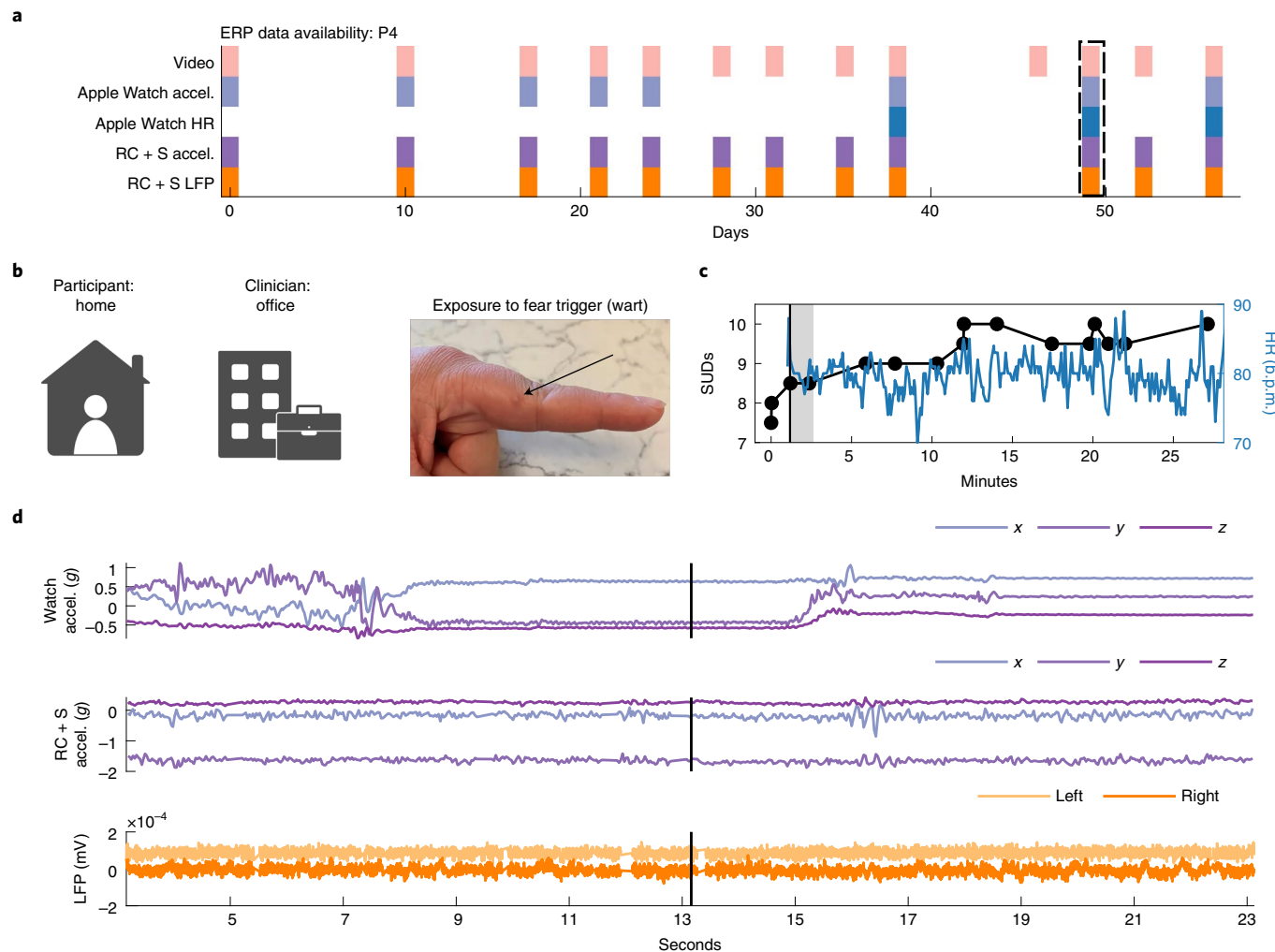


Fig. 5 | Intracranial electrophysiology during exposure and response prevention teletherapy at home with participant P4. **a**, Calendar availability plot of ERP sessions for participant P4, over days since the first ERP session. Shaded portions indicate data availability for ERP video, Apple Watch heart rate, Apple Watch acceleration, RC + S acceleration and RC + S LFP recordings. Rectangular dashed line corresponds to the ERP session example data in **b-d**. **b**, Videos of participant P4 (left) and clinician (center) and image of exposure (right). **c**, Time-course analysis in minutes of self-reported SUD ratings and heart rate collected via the Apple Watch throughout the ERP session. The vertical black line denotes the start of the exposure period. The gray shaded area corresponds to the time period shown in Supplementary Video 2. **d**, 20 s of example data synchronized to video, including Apple Watch acceleration, RC + S acceleration and two bipolar LFP channels. The vertical black line corresponds to the video frame shown in **b**.

biomarkers may not pertain to symptoms but instead to cognitive domains where function may be impaired. Administration of behavioral tasks allows for orthogonalization onto neurobiological axes (that is, the Research Domain Criteria) that could provide useful information for relating mental processes to electrophysiology^{33,34}. Once task-related electrophysiological signatures are identified, it will be important to explore recurrences of task-related neural states in non-task-locked, real-world behavior³⁵. For example, if cognitive control signals are insufficient, stimulation amplitude could be increased to improve decision-making capacity^{36–38}.

Changing DBS parameters and electrode impedance over time will present challenges in neural data interpretation. Even relatively small changes in impedance have been shown to affect the spectral power distribution³⁹. Further, variability in sensing and stimulating contact placement will likely lead to inconsistent neural activity across participants^{40–42}. Here, all five participants had the deepest portion of the leads anchored in gray matter (VS or BNST; Fig. 2 and Extended Data Fig. 1). The stimulation contacts were the second deepest contact on the lead, flanked by sensing contacts. Therefore, the deepest sensing contact in each bipolar pair is likely

sensing neural activity from gray matter, whereas the other contact in the pair is likely sensing neural activity from white matter. LFPs from pure white matter are notoriously difficult to interpret⁴³; however, it is unknown how heavily influenced the recorded voltages are by gray and white matter VS activity. Nevertheless, the gray-white bipolar sensing contact pairs undoubtedly led to caveats in the interpretation of our neural recordings.

The DBS implants used in our study allow for real-time frequency-domain analysis of electrophysiological activity recorded simultaneously during stimulation delivery from the implanted electrodes²⁰. If a reliable relationship between participant state (severity of symptoms or adverse effects) and electrophysiology can be determined, computational methods can produce a classifier that identifies participant state based on measured activity. ‘Untethered’, embedded aDBS solutions are limited by onboard feature estimation and classification capabilities. For example, when embedded on an implanted device, the device can adjust its output based on LFP spectral power in predefined spectral bands used as inputs to a linear discriminant classifier²⁰. While we observed correlations between power in various frequency bands and OCD symptom intensity,

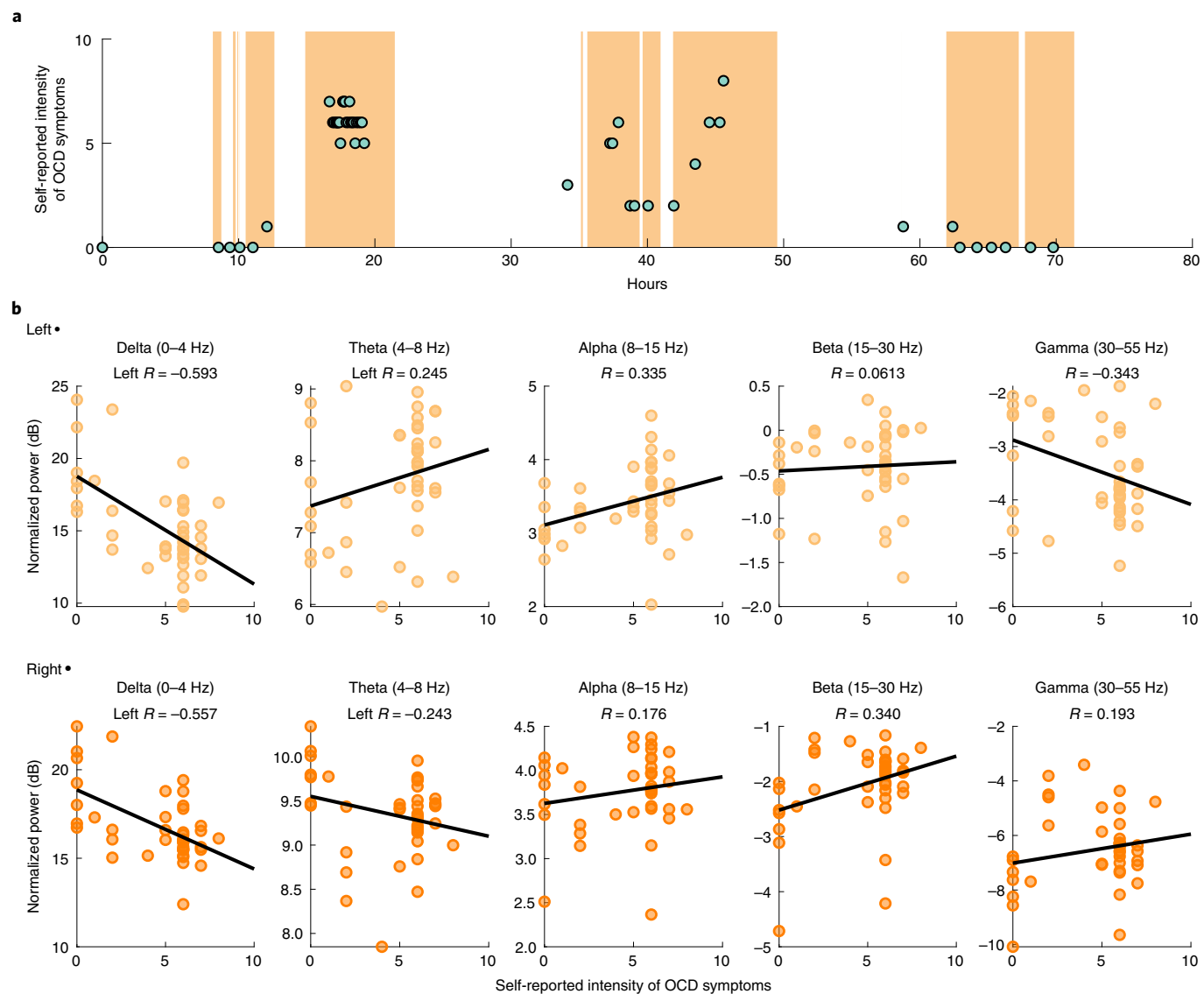


Fig. 6 | Ventral capsule/ventral striatum spectral power shows correlations with obsessive-compulsive disorder symptom intensity during P4 natural exposures at home. **a**, Self-reported intensity of OCD symptoms (scatter points) shown over time (hours) with LFP data availability (orange shading). **b**, Normalized left (top row) and right (bottom row) VC/VS spectral power in delta (0–4 Hz), theta (4–8 Hz), alpha (8–15 Hz), beta (15–30 Hz) and gamma (30–55 Hz; from left to right) versus self-reported OCD symptom intensity from 0 to 10. Black lines represent the least-squares fits. R values correspond to the coefficient of correlation.

additional data collection and analysis are required to validate this finding in a larger sample. As putative biomarkers are identified, further work will be necessary to determine if biomarker-controlled adjustments in stimulation parameters result in an increased therapeutic effect of DBS.

Evidence from tractographic and functional imaging studies suggests that the pathophysiology of OCD does not lie in the VC/VS alone, but rather in the cortico-striatal-thalamo-cortical (CSTC) network^{44,45}. One front-running hypothesis is that DBS acts to disrupt pathological frontostriatal hyperconnectivity in OCD. Several studies, via functional imaging⁴⁶ and intracranial electrophysiology⁴⁷, have shown evidence toward this hypothesis. Few studies report on oscillatory activity in the VC/VS to date, including in cohorts of patients with obesity⁴⁸, addiction⁴⁹, treatment-resistant depression^{50,51} and OCD^{51–54}. While no convergence on an oscillatory biomarker of OCD symptoms across these studies exists, there is promising evidence that VC/VS oscillatory activity may be correlated with behaviors including reward anticipation^{48,50}, error

monitoring⁴⁹ and OCD symptom provocation^{52,54}. Chronic, ecologically valid, VC/VS recordings in humans may provide opportunities to identify a robust candidate biomarker for OCD symptoms.

For our approach to be optimally useful in the treatment of obsessive-compulsive symptoms, we must better understand frontostriatal network activity. Obsessive-compulsive behaviors implicate symptomatic networks. OCD stimulation targets are anatomically linked to structures including the orbitofrontal cortex, the anterior cingulate cortex, the mediodorsal thalamic nucleus and the ventral pallidum^{44,45,55,56}. Stimulation to these targets impacts distributed network-wide activity and has been found to restore frontostriatal network activity in OCD⁴⁶. Physiological studies point to relationships between frontostriatal activity and abnormal reward processing^{40,57}, cognitive flexibility⁵⁸ and decision-making⁵⁹, which are mental processes related to OCD symptoms. Further, connectivity with the prefrontal cortex/supplementary motor area has been shown to be correlated with improvement in OCD symptoms^{47,53,60}. This literature supports the notion that symptoms arise from

network phenomena and motivates the need for both cortical and subcortical inputs as well as simultaneous chronic, intracortical recordings to replicate findings in ecologically valid environments. To best understand the network, technical innovation must include the capacity to record in a few key areas in addition to the VC/VS, including the orbitofrontal cortex or the anterior cingulate cortex.

Finally, we note that the data collection platform presented here could be used in many other contexts beyond DBS programming sessions, daily activities at home and ERP teletherapy for neuropsychiatric patients. To identify robust electrophysiological biomarkers for any psychiatric illness, data must be captured and explored for a vast array of behaviors and contexts. Wireless streaming of neural data enables capture of intracranial electrophysiology data during naturalistic states, including sleep, socialization, eating and exercise. The platform presented here lays the groundwork for future transformational studies reliant on ecological neural and behavioral monitoring and assessment of neuropsychiatric illness.

Online content

Any methods, additional references, Nature Research reporting summaries, source data, extended data, supplementary information, acknowledgements, peer review information; details of author contributions and competing interests; and statements of data and code availability are available at <https://doi.org/10.1038/s41591-021-01550-z>.

Received: 8 March 2021; Accepted: 22 September 2021;

Published online: 09 December 2021

References

- Goodman, W. K., Storch, E. A. & Sheth, S. A. Harmonizing the neurobiology and treatment of obsessive-compulsive disorder. *Am. J. Psychiatry* **178**, 17–29 (2021).
- Pallanti, S., Hollander, E. & Goodman, W. K. A qualitative analysis of nonresponse: management of treatment-refractory obsessive-compulsive disorder. *J. Clin. Psychiatry* **65**, 6–10 (2004).
- Alonso, P. et al. Deep brain stimulation for obsessive-compulsive disorder: a meta-analysis of treatment outcome and predictors of response. *PLoS ONE* **10**, e0133591 (2015).
- Goodman, W. K. et al. Deep brain stimulation for intractable obsessive compulsive disorder: pilot study using a blinded, staggered-onset design. *Biol. Psychiatry* **67**, 535–542 (2010).
- Ooms, P. et al. Deep brain stimulation for obsessive-compulsive disorders: long-term analysis of quality of life. *J. Neurol. Neurosurg. Psychiatry* **85**, 153–158 (2014).
- Denys, D. et al. Efficacy of deep brain stimulation of the ventral anterior limb of the internal capsule for refractory obsessive-compulsive disorder: a clinical cohort of 70 patients. *Am. J. Psychiatry* **177**, 265–271 (2020).
- Okun, M. S. & Foote, K. D. Parkinson's disease DBS: what, when, who and why? the time has come to tailor DBS targets. *Expert Rev. Neurother.* **10**, 1847–1857 (2010).
- Angst, J. et al. Obsessive-compulsive severity spectrum in the community: prevalence, comorbidity, and course. *Eur. Arch. Psychiatry Clin. Neurosci.* **254**, 156–164 (2004).
- Graat, I., Figege, M. & Denys, D. The application of deep brain stimulation in the treatment of psychiatric disorders. *Int. Rev. Psychiatry* **29**, 178–190 (2017).
- Widge, A. S. et al. Treating refractory mental illness with closed-loop brain stimulation: progress towards a patient-specific transdiagnostic approach. *Exp. Neurol.* **287**, 461–472 (2017).
- Provenza, N. R. et al. The case for adaptive neuromodulation to treat severe intractable mental disorders. *Front. Neurosci.* **13**, 152 (2019).
- Little, S. et al. Bilateral adaptive deep brain stimulation is effective in Parkinson's disease. *J. Neurol. Neurosurg. Psychiatry* **87**, 717–721 (2016).
- Swann, N. C. et al. Adaptive deep brain stimulation for Parkinson's disease using motor cortex sensing. *J. Neural Eng.* **15**, 046006 (2018).
- Bergey, G. K. et al. Long-term treatment with responsive brain stimulation in adults with refractory partial seizures. *Neurology* **84**, 810–817 (2015).
- Opri, E. et al. Chronic embedded cortico-thalamic closed-loop deep brain stimulation for the treatment of essential tremor. *Sci. Transl. Med.* **12**, eaay7680 (2020).
- Bouthour, W. et al. Biomarkers for closed-loop deep brain stimulation in Parkinson disease and beyond. *Nat. Rev. Neurol.* **15**, 343–352 (2019).
- Wingeier, B. et al. Intra-operative STN DBS attenuates the prominent beta rhythm in the STN in Parkinson's disease. *Exp. Neurol.* **197**, 244–251 (2006).
- Bijanki, K. R. et al. Cingulum stimulation enhances positive affect and anxiolysis to facilitate awake craniotomy. *J. Clin. Invest.* **129**, 1152–1166 (2019).
- Fullana, M. A. et al. Diagnostic biomarkers for obsessive-compulsive disorder: a reasonable quest or ignis fatuus? *Neurosci. Biobehav. Rev.* **118**, 504–513 (2020).
- Stanslaski, S. et al. A chronically implantable neural coprocessor for investigating the treatment of neurological disorders. *IEEE Trans. Biomed. Circuits Syst.* **12**, 1230–1245 (2018).
- Sun, F. T. & Morrell, M. J. The RNS system: responsive cortical stimulation for the treatment of refractory partial epilepsy. *Expert Rev. Med. Devices* **11**, 563–572 (2014).
- Kremen, V. et al. Integrating brain implants with local and distributed computing devices: a next-generation epilepsy management system. *IEEE J. Transl. Eng. Health Med.* **6**, 2500112 (2018).
- Topalovic, U. et al. Wireless programmable recording and stimulation of deep brain activity in freely moving humans. *Neuron* **108**, 322–334 (2020).
- Gilron, Roee et al. Long-term wireless streaming of neural recordings for circuit discovery and adaptive stimulation in individuals with Parkinson's disease. *Nat. Biotechnol.* <https://doi.org/10.1038/s41587-021-00897-5> (2021).
- Storch, E. A. et al. Defining clinical severity in adults with obsessive-compulsive disorder. *Compr. Psychiatry* **63**, 30–35 (2015).
- Ertugrul, I. O., Jeni, L. A., Ding, W. & Cohn, J. F. AFAR: a deep learning-based tool for automated facial affect recognition. *Proc. Int. Conf. Autom. Face Gesture Recognit.* <https://doi.org/10.1109/FG.2019.8756623> (2019).
- Gibson, W. S. et al. The impact of mirth-inducing ventral striatal deep brain stimulation on functional and effective connectivity. *Cereb. Cortex* **27**, 2183–2194 (2017).
- Nicole R. Provenza, et al. Honeycomb: a template for reproducible psychophysiological tasks for clinic, laboratory, and home use. *Braz. J. Psychiatry* <https://doi.org/10.1590/1516-4446-2020-1675> (2021).
- Mataix-Cols, D. et al. Symptom stability in adult obsessive-compulsive disorder: data from a naturalistic two-year follow-up study. *Am. J. Psychiatry* **159**, 263–268 (2002).
- Nota, J. A., Gibb, B. E. & Coles, M. E. Obsessions and time of day: a self-monitoring study in individuals with obsessive-compulsive disorder. *J. Cogn. Psychother.* **28**, 134–144 (2014).
- Gerald, J. H. & George, S. H. Self-report: psychology's four-letter word. *Am. J. Psychol.* **123**, 181–188 (2010).
- Powers, R. et al. Smartwatch inertial sensors continuously monitor real-world motor fluctuations in Parkinson's disease. *Sci. Transl. Med.* **13**, eabd7865 (2021).
- Cuthbert, B. N. & Insel, T. R. Toward the future of psychiatric diagnosis: the seven pillars of RDoC. *BMC Med.* **11**, 126 (2013).
- Gillan, C. M., Kosinski, M., Whelan, R., Phelps, E. A. & Daw, N. D. Characterizing a psychiatric symptom dimension related to deficits in goal-directed control. *Elife* **5**, e11305 (2016).
- Provenza, N. R. et al. Decoding task engagement from distributed network electrophysiology in humans. *J. Neural Eng.* **16**, 056015 (2019).
- Widge, A. S. et al. Deep brain stimulation of the internal capsule enhances human cognitive control and prefrontal cortex function. *Nat. Commun.* **10**, 1536 (2019).
- Basu, I. et al. Closed loop enhancement and neural decoding of human cognitive control. Preprint at <https://doi.org/10.1101/2020.04.24.059964> (2020).
- Smith, E. H. et al. Widespread temporal coding of cognitive control in the human prefrontal cortex. *Nat. Neurosci.* **22**, 1883–1891 (2019).
- Ung, H. et al. Intracranial EEG fluctuates over months after implanting electrodes in human brain. *J. Neural Eng.* **14**, 056011 (2017).
- Grover, S., Nguyen, J. A., Viswanathan, V. & Reinhart, R. M. G. High-frequency neuromodulation improves obsessive-compulsive behavior. *Nat. Med.* **27**, 232–238 (2021).
- Scangos, K. W., Makhoul, G. S., Sugrue, L. P., Chang, E. F. & Krystal, A. D. State-dependent responses to intracranial brain stimulation in a patient with depression. *Nat. Med.* <https://doi.org/10.1038/s41591-020-01175-8> (2021).
- Figege, M. & Mayberg, H. The future of personalized brain stimulation. *Nat. Med.* <https://doi.org/10.1038/s41591-021-01243-7> (2021).
- Mercier, M. R. et al. Evaluation of cortical local field potential diffusion in stereotactic electro-encephalography recordings: a glimpse on white matter signal. *Neuroimage* **147**, 219–232 (2017).
- Haber, S. N., Yendiki, A. & Jbabdi, S. Four deep brain stimulation targets for obsessive-compulsive disorder: are they different? *Biol. Psychiatry* <https://doi.org/10.1016/j.biopsych.2020.06.031> (2020).
- Li, N. et al. A unified connectomic target for deep brain stimulation in obsessive-compulsive disorder. *Nat. Commun.* <https://doi.org/10.1038/s41467-020-16734-3> (2021).

46. Figuee, M. et al. Deep brain stimulation restores frontostriatal network activity in obsessive-compulsive disorder. *Nat. Neurosci.* **16**, 386–387 (2013).
47. Olsen, S. T. et al. Case report of dual-site neurostimulation and chronic recording of cortico-striatal circuitry in a patient with treatment refractory obsessive compulsive disorder. *Front. Hum. Neurosci.* **14**, 569973 (2020).
48. Wu, H. et al. Closing the loop on impulsivity via nucleus accumbens delta-band activity in mice and man. *Proc. Natl Acad. Sci. USA* **115**, 192–197 (2018).
49. Sildatke, E. et al. Error-related activity in striatal local field potentials and medial frontal cortex: evidence from patients with severe opioid abuse disorder. *Front. Hum. Neurosci.* **14**, 627564 (2020).
50. Lega, B. C., Kahana, M. J., Jaggi, J., Baltuch, G. H. & Zaghloul, K. Neuronal and oscillatory activity during reward processing in the human ventral striatum. *Neuroreport* **22**, 795–800 (2011).
51. Neumann, W.-J. et al. Different patterns of local field potentials from limbic DBS targets in patients with major depressive and obsessive compulsive disorder. *Mol. Psychiatry* **19**, 1186–1192 (2014).
52. Miller, K. J., Prieto, T., Williams, N. R. & Halpern, C. H. Case Studies in neuroscience: the electrophysiology of a human obsession in nucleus accumbens. *J. Neurophysiol.* **121**, 2336–2340 (2019).
53. Schwabe, K. et al. Oscillatory activity in the BNST/ALIC and the frontal cortex in OCD: acute effects of DBS. *J. Neural Transm.* <https://doi.org/10.1007/s00702-020-02297-6> (2021).
54. Frank, A. C. et al. Identification of a personalized intracranial biomarker of depression and response to DBS therapy. *Brain Stimul.* **14**, 1002–1004 (2021).
55. Tyagi, H. et al. A randomized trial directly comparing ventral capsule and anteromedial subthalamic nucleus stimulation in obsessive-compulsive disorder: clinical and imaging evidence for dissociable effects. *Biol. Psychiatry* **85**, 726–734 (2019).
56. Liebrand, L. C. et al. Individual white matter bundle trajectories are associated with deep brain stimulation response in obsessive-compulsive disorder. *Brain Stimul.* **12**, 353–360 (2019).
57. Figuee, M. et al. Dysfunctional reward circuitry in obsessive-compulsive disorder. *Biol. Psychiatry* **69**, 867–874 (2011).
58. Eijker, N., van Wingen, G., Smolders, R., Smit, D. J. A. & Denys, D. Exploring the role of the nucleus accumbens in adaptive behavior using concurrent intracranial and extracranial electrophysiological recordings in humans. *eNeuro* **7**, ENEURO.0105-20.2020 (2020).
59. Stenner, M.-P. et al. Cortical drive of low-frequency oscillations in the human nucleus accumbens during action selection. *J. Neurophysiol.* **114**, 29–39 (2015).
60. Smith, E. E. et al. A brief demonstration of frontostriatal connectivity in OCD patients with intracranial electrodes. *Neuroimage* **220**, 117138 (2020).

Publisher's note Springer Nature remains neutral with regard to jurisdictional claims in published maps and institutional affiliations.

This is a U.S. government work and not under copyright protection in the U.S.; foreign copyright protection may apply 2021

Methods

Study design. An early feasibility study of aDBS was conducted in adults with severe and intractable OCD (NCT04281134 and NCT03457675). Participants entered a 6-month trial of open-label bilateral DBS targeting the VC/VS followed by 2 months of adjunctive ERP therapy. Subsequently, they entered a blinded discontinuation period to assess the need for ongoing DBS. The primary clinical outcome measure was change in the Y-BOCS scores, where a 35% reduction from baseline defined participants as ‘responders’.

To date, five adults with a principal diagnosis of severe and intractable OCD underwent DBS surgery after being apprised of the risks, possible benefits and alternatives to participation in the research study. All participants had OCD for more than 5 years and failed, or were unable to tolerate, adequate trials of multiple medications (that is, selective serotonin reuptake inhibitors (SSRIs), clomipramine and SSRI plus antipsychotics), as well as a course of ERP. Two participants (P1, 31M; P2, 39F) were implanted with the Activa PC+S (Medtronic) device, and three participants (P3, 37F; P4, 40M; P5, 31F) were implanted with the Summit RC+S (Medtronic) device. Each participant gave fully informed consent according to study sponsor guidelines, and all procedures were approved by the local institutional review board at Baylor College of Medicine (H-40255 and H-44941 to Baylor College of Medicine, IAA 17–27 and IAA 19–51 to Brown University, and STUDY20110082 and STUDY20110084 to University of Pittsburgh) and the US Food and Drug Administration Center for Devices and Radiological Health. Participants received a stipend after each study visit via a ClinCard.

DBS surgery. DBS leads (model 3387) were placed bilaterally in the VC/VS region. Lead locations were determined using direct targeting on the preoperative MRI: we targeted the gray-white interface in the ventral region of the anterior limb of the internal capsule. We created two trajectories per hemisphere, one immediately anterior and one immediately posterior to the AC. We conceive of these targets not as different regions but rather as two anatomical methods to find the optimal, individual-specific target within the same ‘VC/VS region’, consistent with recent connectomic studies⁴⁴. We refer to the anterior target as the ‘VC/VS’ per se, as the VS is the gray matter immediately subjacent. We refer to the posterior target as the BNST, which is immediately subjacent.

We used the observation of a ‘mirth’ or ‘positive valence’ response during intraoperative testing as an indicator of which location within the broader VC region would be more promising for eventual symptomatic improvement. Our decision to evaluate therapeutic response to DBS on both sides of the AC was driven by empirical evidence from the literature that more posterior targets lead to better outcomes. This effect may be related to the distribution of the passing fibers that fan out and diverge at the AC, which has been characterized via tractography and can vary for individual patients^{44,45}. There is tractographic evidence that this positive mood response is due to DBS engagement of tracts that are more ventral, including the anterior cingulate cortex, orbitofrontal cortex and ventromedial prefrontal cortex⁵⁶. We think of positive valence activation as a guidepost, as it may indicate that DBS is engaging the ventral limbic tracts that are associated with OCD.

The leads were connected to extensions, tunneled down the neck, and connected to the Activa PC+S or Summit RC+S placed in the upper left of the chest to enable wireless streaming of LFP data. P1, P3, P4 and P5 received bilateral stimulation, and P2 received unilateral stimulation.

Clinical assessments. The Y-BOCS and Y-BOCS II⁶¹ were administered during clinical visits before DBS programming sessions. The Y-BOCS is the gold-standard clinician-administered tool for measuring severity of OCD and assessing treatment response^{62,63}. The Y-BOCS II is a modified version of the original Y-BOCS that was designed to be more sensitive to changes in symptom severity among patients with very severe OCD⁶¹.

MRI protocol. Preoperative MRI was performed on a Siemens Prisma 3T scanner with a 64-channel head-neck coil. High-resolution (0.8 mm isotropic) T1w anatomical images (MPRAGE; repetition time (TR) of 2,400 ms, time echo (TE) of 2.24 ms, an inversion time (TI) of 1,000 ms, a flip angle of 8° and an acquisition time (TA) of ~7 min) were acquired. T2-weighted (T2w) images (SPACE; 0.8 mm isotropic; TR of 3,200 ms, TE of 563 ms and a TA of ~6 min) were acquired in the same session.

Computed tomography imaging. In addition, the participants underwent preoperative clinical computerized tomography (CT) acquisition with contrast, as well as postoperative clinical CT acquisition to confirm electrode implant locations. The postoperative CT data were registered to the T1w MRI space and were used to extract the contact positions relative to local neuroanatomy.

Cortical reconstructions. An automatic cortical reconstruction was performed on the preoperative T1w MRI using FreeSurfer v7.1.1 (<https://surfer.nmr.mgh.harvard.edu/>)⁶⁴ and the T2w MRI was used to improve reconstruction of the pial surfaces. The postoperative CT data were aligned to the preoperative T1w MRI using the Functional Magnetic Resonance Imaging for the Brain Software Library’s Linear Image Registration Tool (v6.0)^{65,66}. Electrode coordinates were manually determined from the co-registered CT data in BioImage Suite v3.5b1 (ref. ⁶⁷) and

placed into the native MRI space. The reconstructed cortical surface (pial surface), segmented subcortical structures and electrode coordinates were visualized using the Multi-Modal Visualization Tool^{68,69}. The caudate, putamen and the VS were colored on the T1w slice based on the subcortical segmentation. The AC was manually reconstructed by tracing the white fiber tracts on the T1w MRI slice.

Medtronic Summit RC+S research platform. Herein, we concentrate on data gathered from the three participants who were implanted with the Summit RC+S system as it allows for extensive home recordings not possible with the Activa PC+S system. The Summit RC+S INS enables both neurostimulation and continuous telemetry of intracranial LFP and accelerometry. The Clinician Telemetry Module enables bidirectional communication between the INS (via telemetry) and a custom-built application developed with the Research Development Kit (via Bluetooth to a separate host computer). The Surface Pro and Surface Go tablets were used in the clinic and at home to deploy the custom-built clinician and patient-facing applications that interface with the INS and cloud (<https://www.box.com/>) to create a flexible platform for data collection and storage. During recording sessions, the Clinician Telemetry Module must be within arm’s reach (1 m) of the INS, and the host computer must be within the same room.

Summit RC+S DBS programming session protocol. Summit RC+S recordings during DBS programming sessions in the clinic were conducted using a clinician-facing application that communicates with the Medtronic Summit application programming interface running on a Surface Pro tablet (<https://github.com/openmind-consortium/App-aDBS-ResearchFacingApp/>). The application allows for changes in bipolar sensing contact configuration, stimulation groups and stimulation parameters including amplitude, pulse width and rate within previously defined safe boundaries set by the clinician using the Medtronic Research Lab Programmer. Starting a recording session triggered sensing from two LFP channels and xyz acceleration.

DBS parameter optimization is completed solely on the basis of clinical evaluation, including standardized clinical assessments (for example, Y-BOCS), interactions with the participants and their family members, and subjective participant reports of changes in mood, anxiety and alertness during acute DBS programming. To determine optimal stimulation parameters, the clinician adjusted one stimulation parameter at a time (either amplitude or pulse width), pausing to assess the participant’s mood and symptoms after each change.

In addition to Summit RC+S recordings, additional multimodal electrophysiological recordings were conducted simultaneously during DBS programming sessions. These recordings included a video of the face to enable AFAR and estimation of head velocity, EEG, ECG and BVP, and are further described below.

At-home recording session protocol. Study participants implanted with the RC+S (P3, P4 and P5) agreed to participate in electrophysiological recordings, momentary self-report behavioral assessments and behavioral tasks in their home environments.

Participants started their own recording sessions using a patient-facing application (frontend, <https://github.com/openmind-consortium/App-OCD-PatientFrontend/>; backend, <https://github.com/openmind-consortium/App-OCD-PatientBackend/>) that communicates with the Medtronic Summit application programming interface. To start a recording, the participant opened the application, and pressed a button on the user interface labeled ‘record’. Pressing the ‘record’ button triggered sensing from two LFP channels and xyz acceleration. Stimulation parameters were constant throughout each recording at home. The StriveStudy mobile application was also used to collect heart rate and acceleration data via an Apple Watch.

Protocols for the three different types of recordings (daily, task and sprint) that the participants were asked to complete at home is further described below.

Daily recordings. Participants were asked to complete at least one 30-min recording session per day during unstructured daily activities at home, with 1 d off each week. Before each recording session, participants were asked to complete a momentary self-reported behavioral assessment.

Momentary self-reported behavioral assessments. Participants used the StriveStudy mobile application (Rune Labs) to report their OCD symptom intensity on a scale from zero to ten, where zero corresponds to ‘very slightly or not at all’, five corresponds to ‘moderately’ and ten corresponds to ‘extreme’. Due to the highly yoked nature of obsessive-compulsive symptoms, OCD symptom intensity ratings did not distinguish between obsessions and compulsions. The Rune Labs mobile application was deployed at the following times: 0 weeks since DBS ON in P3, 13 weeks since DBS ON in P4 and 4 weeks before DBS ON in P5.

Task recordings. Participants were asked to complete behavioral tasks during a recording session one time each week. Behavioral tasks included the multisource interference task for assessing cognitive control and cognitive flexibility (<https://github.com/brown-ccv/task-msit>)^{70,71}, the beads task for assessing intolerance to uncertainty and sensitivity to reward adapted from work by Voon et. al⁷², and the

resting-state task to gauge brain activity at rest (<https://github.com/brown-ccv/task-resting-state/>). Tasks were all developed using Honeycomb, a template for reproducible behavioral tasks for clinic, laboratory and home use (<https://github.com/brown-ccv/honeycomb/>)²⁸. Honeycomb allows for flexible task deployment with and without external electrophysiological recordings, and enabled our experiments to be conducted both in research settings and at home.

Sprint recordings. Participants were asked to engage in multiday ‘sprint’ recordings (that is, multi-hour recording sessions). During the sprint recordings, participants were asked to use the StriveStudy mobile application to report their OCD symptom intensity on an hourly basis.

Exposure and response prevention therapy recordings. Participants engaged in a course of ERP teletherapy (13 to 14 appointments) from approximately 10 to 12 months after DBS was turned on. Participants were asked to start a recording session at the beginning of the appointment, and video recordings were saved to the clinician’s computer using Zoom Video Communications.

Local field potential recordings. LFPs were sampled at a rate of 200 Hz (Activa PC + S) or 1,000 Hz (Summit RC + S) in the clinic, and 250 Hz (Summit RC + S) at home. LFPs were sensed in bipolar configuration, meaning that a pair of sensing contacts was selected on each lead so that the signal recorded by one sensing contact was referenced to the other in the pair. Sensing and stimulation contact information for each participant is provided in Supplementary Table 1. To reduce DBS-related artifacts, the sensing contact pair was configured to flank the stimulation contact when possible. The low-pass filter stage 1 and 2 cutoff frequencies were both set to 100 Hz to further minimize impact of stimulation artifacts on the recorded signal. The high-pass filter cutoff frequency was set to 0.85 Hz. All sensing was conducted using active recharge stimulation. Acceleration in the *x*, *y* and *z* axes was also measured onboard the Summit RC + S device by an accelerometer located in the case.

Electroencephalography and peripheral electrophysiology recordings. EEG was recorded during programming sessions and behavioral tasks in the clinic using a 64-channel active-electrode cap (actiCAP slim, Brain Products) and amplifiers (BrainAmp MR Plus) with an online reference at electrode FCz. Event markers were recorded along with EEG data using a TriggerBox (Brain Products) as well as a photodiode. EEG data were sampled at 5 kHz with a high cutoff at 1,000 Hz using the BrainVision recorder. Three-lead ECG and BVP were connected to the BrainAmp ExG amplifier. ECG leads were connected to just above and below the left pectoral muscle, grounded to below the right pectoral. The BVP sensor was clipped onto the index finger of the nondominant hand.

Audio and video recordings. Video and audio were recorded using the GoPro Hero 6 at 25 f.p.s., and an external microphone (Zoom H4n Pro 4-Track Portable Recorder) at 44.1 kHz. High-quality audio was synchronized with video by cross correlating the low-quality and high-quality audio tracks recorded by the GoPro Hero 6 and external microphone, respectively. Then the original audio was removed from the video and replaced by the high-quality audio.

Remote data management. Data from the Summit RC + S patient-facing application and behavioral task data were automatically uploaded to <https://www.box.com/> from Surface Go tablets via a .BAT script triggered by Windows task scheduler upon connecting to the internet or by the user logging in or out (<https://github.com/neuromotion/rfps-box-upload/>).

Data synchronization: EEG to local field potentials. LFP and EEG data were synchronized by identifying features common to both recordings. Sequences of 5-Hz pulses were briefly applied at the beginning and end of each recording session. These pulses are visible in both the LFP and EEG recordings due to the high amplitude of the stimulation artifacts they produce. Corresponding pulses were identified in both recordings and used as alignment points.

Data synchronization: EEG to task (in-clinic). The start and end times of DBS programming sessions were marked in the EEG recording using a ‘pseudo-behavioral task’ consisting solely of a start/stop button. Pressing the start and stop button in the task triggered a serial event message that was sent from the Surface Pro tablet to the BrainVision EEG amplifier via the TriggerBox.

Data synchronization: EEG to video. The pseudo-behavioral task also triggered a unique audible tone at the same time that the serial event was sent. This tone was recorded by both the GoPro video camera and external microphone. The tone was identified algorithmically in each audio file using the MATLAB function ‘findsignal’, and the time point of the tone was used as the synchronization point between audio/video and EEG recordings.

Data synchronization: intracranial electrophysiology to task (at-home). Each behavioral task output a JSON file containing data saved from the task including the Unix time (time of day) when each task event occurred. Task behavior and LFP

were time-stamped using the same clock (Surface Go clock) and therefore could easily be aligned.

Data synchronization: intracranial electrophysiology to Rune StriveStudy mobile application output. LFP Unix time was aligned to OCD symptom intensity rating, Apple Watch acceleration and Apple Watch heart rate Unix time.

Data synchronization: intracranial electrophysiology to ERP video. ERP video recordings were saved with a date and time stamp on each video frame. Time of day from the video was used to align video to LFP Unix time.

Signal reconstruction after packet loss. We accounted for packet losses in LFP data to enable synchronization between LFP and other data streams⁷³. Details and code for the procedure we used are available at <https://github.com/openmind-consortium/Analysis-rcts-data/>.

Artifact removal: low-pass filter. Before filtering, missing LFP samples were replaced with the mean value of the remaining samples. LFP and EEG were then low-pass filtered using a finite impulse response filter between 100 and 130 Hz with 40 dB of attenuation in the stopband and 0.1 dB of passband ripple. The filter was designed using the MATLAB function ‘designfilt’ and applied to the recording using ‘filtfilt’.

Objective, automatic measurement of affective valence and head dynamics. Facial expression of positive and negative valence and the dynamics of head motion were measured using AFAR. AFAR is a computer-vision-based approach that can objectively measure the occurrence, intensity and timing of facial action units^{26,74–76}, head pose⁷⁷ and gaze⁷⁸ at video frame rate (30 to 60 f.p.s.). Action units are anatomically based actions that individually or in combination can describe nearly all possible facial expressions⁷⁹. Previous research has identified action units associated with positive (for example, enjoyment) and negative (for example, fear, anger, disgust and anxiety) emotion^{80–82}, and representations of positive and negative valence and pain^{83–86}. Velocity of head motion has been found to increase with strong negative affect^{87–90} and is inversely related to severity of depression^{91,92}. In preliminary studies, AFAR revealed strong effects of DBS in both intraoperative contexts and interviews^{93,94}.

We measured positive valence on a scale of zero to five as the mean intensity of facial action units 6 and 12. Action unit 6 (orbicularis oculi pars orbitalis) raises the cheeks, narrows the eye aperture laterally and can cause crow’s-feet wrinkles at the eye corners. Action unit 12 (zygomatic major) stretches the lips obliquely and affects shape and appearance of the nasolabial furrows. Head movements were measured by the angular velocity of pitch and yaw head motions in units of degree per second. Head pitch and yaw were smoothed using a 5-s moving average before calculating the frame-to-frame velocity. To aid interpretation, the frame-level velocity was converted to degrees per second. An example of AFAR tracking of positive valence and head velocity is shown in Fig. 3b,c. Participants P4, P5 and an author (A.D.W.) gave informed consent for publication of their images and videos in this paper.

Neural data analysis for sprint and ERP recordings at home. We analyzed one sprint dataset collected at home over multiple days by P4, 531–533 d after DBS surgery. We chose this dataset due to the high variability and large range in self-reported OCD symptom intensity ratings over the 3-d span. Our goal was to characterize how the spectral content of the VC/VS LFP signal was changing with OCD symptom intensity rating.

A total of 41 OCD symptom intensity ratings were reported during LFP recordings over the 3-d span. LFP data were divided into 2-min segments, 1 min before and 1 min after each self-reported OCD symptom intensity rating was logged. Within that time frame, all contiguous segments of data with a duration of 500 ms or more were included in analysis. A Hamming window (MATLAB, hamming) was used to divide the data into 500-ms segments with 250 ms of overlap, and the mean of the entire recording was subtracted from each window to remove DC offset. Power spectral density (PSD) estimates were calculated using the Welch method (MATLAB, pwelch). The median PSD was computed for each 2-min segment. Transient outliers due to motion or background device processes were not explicitly removed but were handled by our choice of using median for central tendency. The median PSD was normalized by dividing by the average power between 4 and 80 Hz.

We then calculated average power in predefined frequency bands of interest (delta, 0–4 Hz; theta, 4–8 Hz; alpha, 8–15 Hz; beta, 15–30 Hz; gamma, 30–55 Hz) by computing the mean power within each frequency band. Resulting values in (mV²/Hz) were converted to decibels, by computing ten times the base-ten logarithmic transform. Therefore, each OCD symptom intensity rating was associated with normalized average power in each predefined frequency band of interest. A line of least squares was fit to each scatterplot (MATLAB, lsline) and the coefficient of correlation (*R*) was computed to measure the strength of the relationship between spectral band power and OCD symptom intensity rating.

Neural data analysis for ERP recordings at home. We repeated the analysis described in the previous section using one ERP dataset for each participant. The

datasets chosen were 232 d after surgery for P3, 278 d after surgery for P4 and 281 d after surgery for P5.

Reporting Summary. Further information on research design is available in the Nature Research Reporting Summary linked to this article.

Data availability

The complete datasets generated (excluding video/audio) and analyzed during the current study will be made publicly available at study completion and will be deposited in the NIH Data Archive for the Brain Initiative. The minimum dataset required to reproduce all results of the paper (excluding video and audio) is publicly available through the associated Open Science Framework project at <https://doi.org/10.17605/OSF.IO/YQA2K>.

Code availability

Custom code used to produce the results in this paper is available at <https://github.com/neuromotion/ecological-ephys-behav-ocd>.

References

61. Storch, E. A. et al. Psychometric analysis of the Yale-Brown Obsessive–Compulsive Scale Second Edition Symptom Checklist. *J. Anxiety Disord.* **24**, 650–656 (2010).
62. Goodman, W. K. et al. The Yale-Brown Obsessive Compulsive Scale. I. Development, use, and reliability. *Arch. Gen. Psychiatry* **46**, 1006–1011 (1989).
63. Goodman, W. K. et al. The Yale-Brown Obsessive Compulsive Scale. II. Validity. *Arch. Gen. Psychiatry* **46**, 1012–1016 (1989).
64. Fischl, B. FreeSurfer. *NeuroImage* **62**, 774–781 (2012).
65. Jenkinson, M. & Smith, S. A global optimisation method for robust affine registration of brain images. *Med. Image Anal.* **5**, 143–156 (2001).
66. Jenkinson, M., Bannister, P., Brady, M. & Smith, S. Improved optimization for the robust and accurate linear registration and motion correction of brain images. *Neuroimage* **17**, 825–841 (2002).
67. Joshi, A. et al. Unified framework for development, deployment and robust testing of neuroimaging algorithms. *Neuroinformatics* **9**, 69–84 (2011).
68. Felsenstein, O. & Peled, N. MMVT-Multi-Modality Visualization Tool. *Github Repository* <https://github.com/pelednoam/mmvt> (accessed June 1, 2020) (2017).
69. Felsenstein, O. et al. Multi-Modal Neuroimaging Analysis and Visualization Tool (MMVT). Preprint at <https://arxiv.org/abs/1912.10079> (2019).
70. Bush, G., Shin, L. M., Holmes, J., Rosen, B. R. & Vogt, B. A. The Multi-Source Interference Task: validation study with fMRI in individual subjects. *Mol. Psychiatry* **8**, 60–70 (2003).
71. Bush, G. & Shin, L. M. The Multi-Source Interference Task: an fMRI task that reliably activates the cingulo-frontal-parietal cognitive/attention network. *Nat. Protoc.* **1**, 308–313 (2006).
72. Voon, V. et al. Decisional impulsivity and the associative-limbic subthalamic nucleus in obsessive-compulsive disorder: stimulation and connectivity. *Brain* **140**, 442–456 (2017).
73. Sellers, K. K. et al. Analysis-rccs-data: open-source toolbox for the ingestion, time-alignment, and visualization of sense and stimulation data from the Medtronic Summit RC+S system. *Front. Hum. Neurosci.* **15**, 714256 (2021).
74. Ertugrul, I. Ö., Yang, L., Jeni, L. A. & Cohn, J. F. D-PAttNet: Dynamic patch-attentive deep network for action unit detection. *Front. Comput. Sci.* **1**, 11 (2019).
75. Niinuma, K., Jeni, L. A., Ertugrul, I. Ö. & Cohn, J. F. Unmasking the devil in the details: what works for deep facial action coding? *BMVC* **4**, (2019).
76. Yang, L. et al. FACS3D-Net: 3D convolution-based spatiotemporal representation for action unit detection. In *8th International Conference on Affective Computing and Intelligent Interaction* <https://doi.org/10.1109/ACII.2019.8925514> (2019).
77. Jeni, L. A., Cohn, J. F. & Kanade, T. Dense 3D face alignment from 2D video for real-time use. *Image Vis. Comput.* **58**, 13–24 (2017).
78. Jeni, L. A. & Cohn, J. F. Person-independent 3D gaze estimation using face frontalization. In *Proceedings of the IEEE conference on computer vision and pattern recognition workshops* 87–95 (2016).
79. Ekman, P., Friesen, W. V. & Hager, J. C. Facial Action Coding System (FACS) (A Human Face, 2002).
80. Ekman, P. & Rosenberg, E. L. *What the Face Reveals: Basic and Applied Studies of Spontaneous Expression Using the Facial Action Coding System (FACS)* (Oxford University Press, 2005).
81. Zhang, Z. et al. Multimodal spontaneous emotion corpus for human behavior analysis. In *Proceedings of the IEEE Conference on Computer Vision and Pattern Recognition* 3438–3446 (2016).
82. Cowen, A. S. et al. Sixteen facial expressions occur in similar contexts worldwide. *Nature* **589**, 251–257 (2021).
83. Baker, J., Haltigan, J. D. & Messinger, D. S. Non-expert ratings of infant and parent emotion: concordance with expert coding and relevance to early autism risk. *Int. J. Behav. Dev.* **34**, 88–95 (2010).
84. Messinger, D. S., Mahoor, M. H., Chow, S.-M. & Cohn, J. F. Automated measurement of facial expression in infant–mother interaction: a pilot study. *Infancy* **14**, 285–305 (2009).
85. Prkachin, K. M. & Solomon, P. E. The structure, reliability and validity of pain expression: evidence from patients with shoulder pain. *Pain* **139**, 267–274 (2008).
86. Haines, N., Southward, M. W., Cheavens, J. S., Beauchaine, T. & Ahn, W.-Y. Using computer-vision and machine learning to automate facial coding of positive and negative affect intensity. *PLoS ONE* <https://doi.org/10.1371/journal.pone.0211735> (2019).
87. Hammal, Z., Cohn, J. F. & George, D. T. Interpersonal coordination of headmotion in distressed couples. *IEEE Trans. Affect. Comput.* **5**, 155–167 (2014).
88. Hammal, Z., Cohn, J. F., Heike, C. & Speltz, M. L. Automatic measurement of head and facial movement for analysis and detection of infants' positive and negative affect. *Front. ICT* **2**, 21 (2015).
89. Hammal, Z., Cohn, J. F. & Messinger, D. S. Head movement dynamics during play and perturbed mother-infant. *Interact. IEEE Trans. Affect. Comput.* **6**, 361–370 (2015).
90. Hammal, Z. et al. Dynamics of face and head movement in infants with and without craniofacial microsomia: an automatic approach. *Plast. Reconstr. Surg. Glob. Open* **7**, e2081 (2019).
91. Dibeklioğlu, H., Hammal, Z. & Cohn, J. F. Dynamic multimodal measurement of depression severity using deep autoencoding. *IEEE J. Biomed. Health Inform.* **22**, 525–536 (2018).
92. Kacem, A., Hammal, Z., Daoudi, M. & Cohn, J. Detecting depression severity by interpretable representations of motion dynamics. *Proc. Int. Conf. Autom. Face Gesture Recognit.* **2018**, 739–745 (2018).
93. Cohn, J. F. et al. Automated affect detection in deep brain stimulation for obsessive-compulsive disorder: a pilot study. *Proc. ACM Int. Conf. Multimodal Interact.* **2018**, 40–44 (2018).
94. Ding, Y. et al. Automated Detection of Optimal DBS Device Settings. *Companion Publ. 2020 Int. Conf. Multimodal Interact.* **2020**, 354–356, 2020.

Acknowledgements

The authors thank the participants and their families for their involvement in the research program. The authors also thank K. Lane for artistic contribution in the creation of Fig. 1. This work relied heavily on the community expertise and resources made available by the Open Mind Consortium (<https://openmind-consortium.github.io/>). Summit RC + S devices were donated by Medtronic as part of the BRAIN Initiative Public-Private Partnership Program. We thank J. Murphy for expertise and contributions in designing and machining equipment used in this study. Part of this research was conducted with the help of research staff at the Center for Computation and Visualization, Brown University (senior research software engineers B. Roarr and M. McGrath). The research was supported by the National Institutes of Health (NIH) NINDS BRAIN Initiative via contracts UH3NS100549 (to S.A.S., J.F.C., D.A.B., E.A.S. and W.K.G.) and UH3NS103549 (to S.A.S.), the Charles Stark Draper Laboratory Fellowship (to N.R.P.), the McNair Foundation (to S.A.S.), the Texas Higher Education Coordinating Board NIH 1RF1MH121371 and U54HD083092 (to E.A.S.), NIH MH096951 (to J.F.C.), K01MH116364 and R21NS104953 (to K.B.), 3R25MH101076-05S2 (to A.B.-A.), award 1S10OD025181 (to J. Sanes at Brown University for computational resources) and the Karen T. Romer Undergraduate Teaching and Research Award at Brown University (E.M.D.-v.R. under the guidance of D.A.B.).

Author contributions

W.K.G., J.F.C., S.A.S. and D.A.B. conceived of the study. N.R.P. conceptualized data analysis procedures, performed data analysis, interpreted data and prepared figures and results with support from E.M.D.-v.R., M.T.H., R.K.M., N.P., Y.D., A.B.-A., S.A.S. and D.A.B. E.M.D.-v.R. carried out packet loss correction and artifact removal procedures with support from N.R.P. and M.T.H. J.X. optimized the MRI protocol. R.K.M., N.P., K.B. and N.R.P. performed MRI analysis, and N.P. developed the Multi-Modal Visualization Tool software. L.A.J. and I.O.E. developed AFAR analysis methodology. Y.D. and L.A.J. performed AFAR analysis, and N.R.P., L.A.J. and Y.D. created the supplementary videos. G.S.V., M.A.-O., N.R. and N.R.P. performed data collection in the clinic. E.R.M. supported data collection. N.R.P., G.S.V. and M.A.-O. guided participant data collection at home. A.D.W. provided clinical ERP sessions, and A.D.W. and N.R.P. collected data during ERP, supervised by E.A.S. A.B.-A. documented SUD ratings using ERP videos. L.F.F.G. and D.X. created new software to enable the collection of intracranial electrophysiological data at home. N.R.P. and S.A.S. wrote the first draft of the manuscript and all authors contributed to the writing and revision of the manuscript. W.K.G., S.A.S., A.V. and E.A.S. performed the clinical care aspects of the study. S.A.S. and A.V. performed the study surgical procedures. W.K.G., S.A.S., J.F.C., E.A.S. and D.A.B. oversaw the collection of data, analysis and manuscript completion.

Competing interests

D.A.B. and W.K.G. received device donations from Medtronic as part of the NIH BRAIN Public-Private Partnership Program. W.K.G. received honoraria from Biohaven Pharmaceuticals. S.A.S. has consulting agreements with Boston Scientific, NeuroPace,

Koh Young, Zimmer Biomet and Abbott. N.P. is a co-founder and stocks holder at FIND Surgical Sciences. The remaining authors declare no competing interests.

Additional information

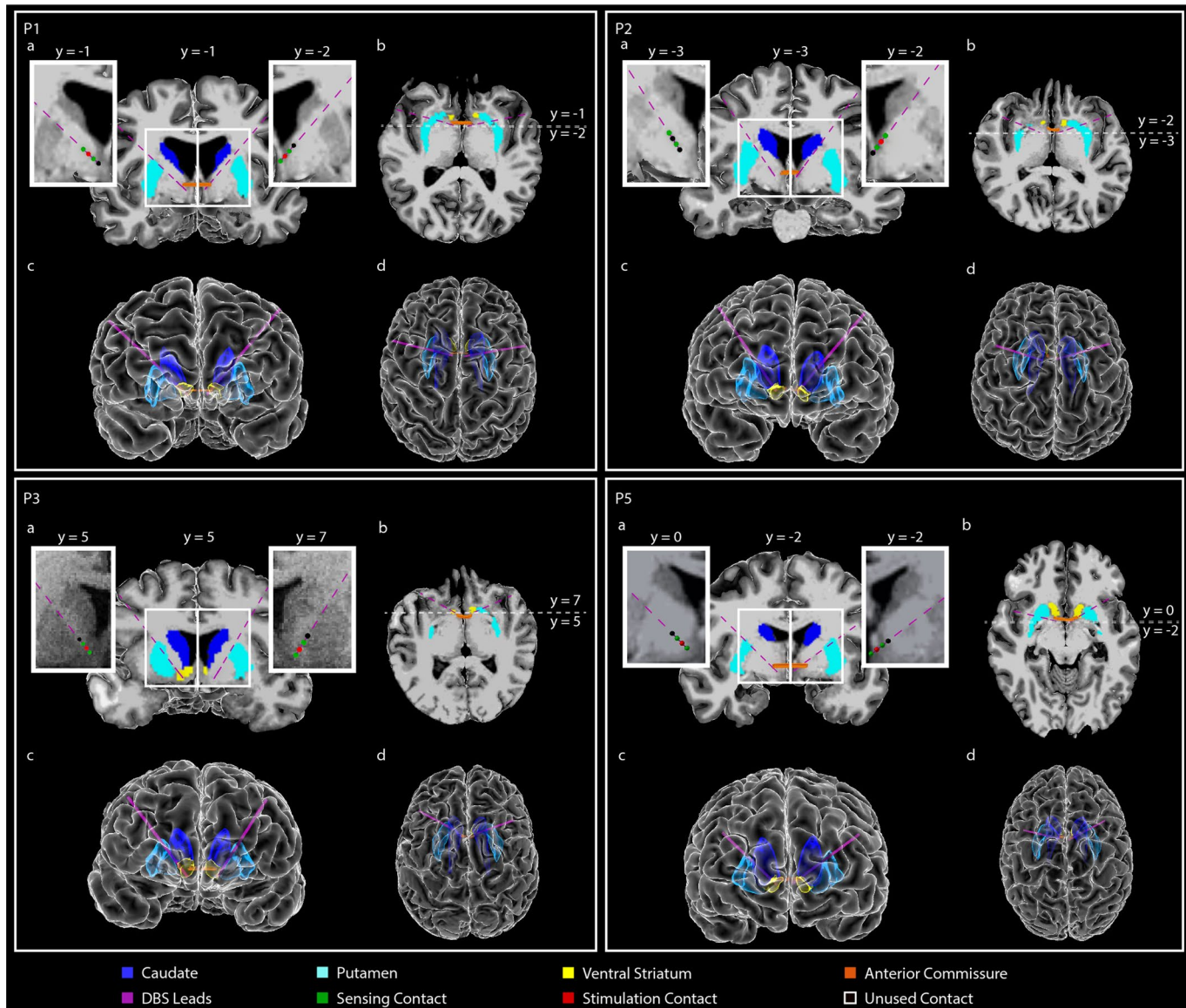
Extended data is available for this paper at <https://doi.org/10.1038/s41591-021-01550-z>.

Supplementary information The online version contains supplementary material available at <https://doi.org/10.1038/s41591-021-01550-z>.

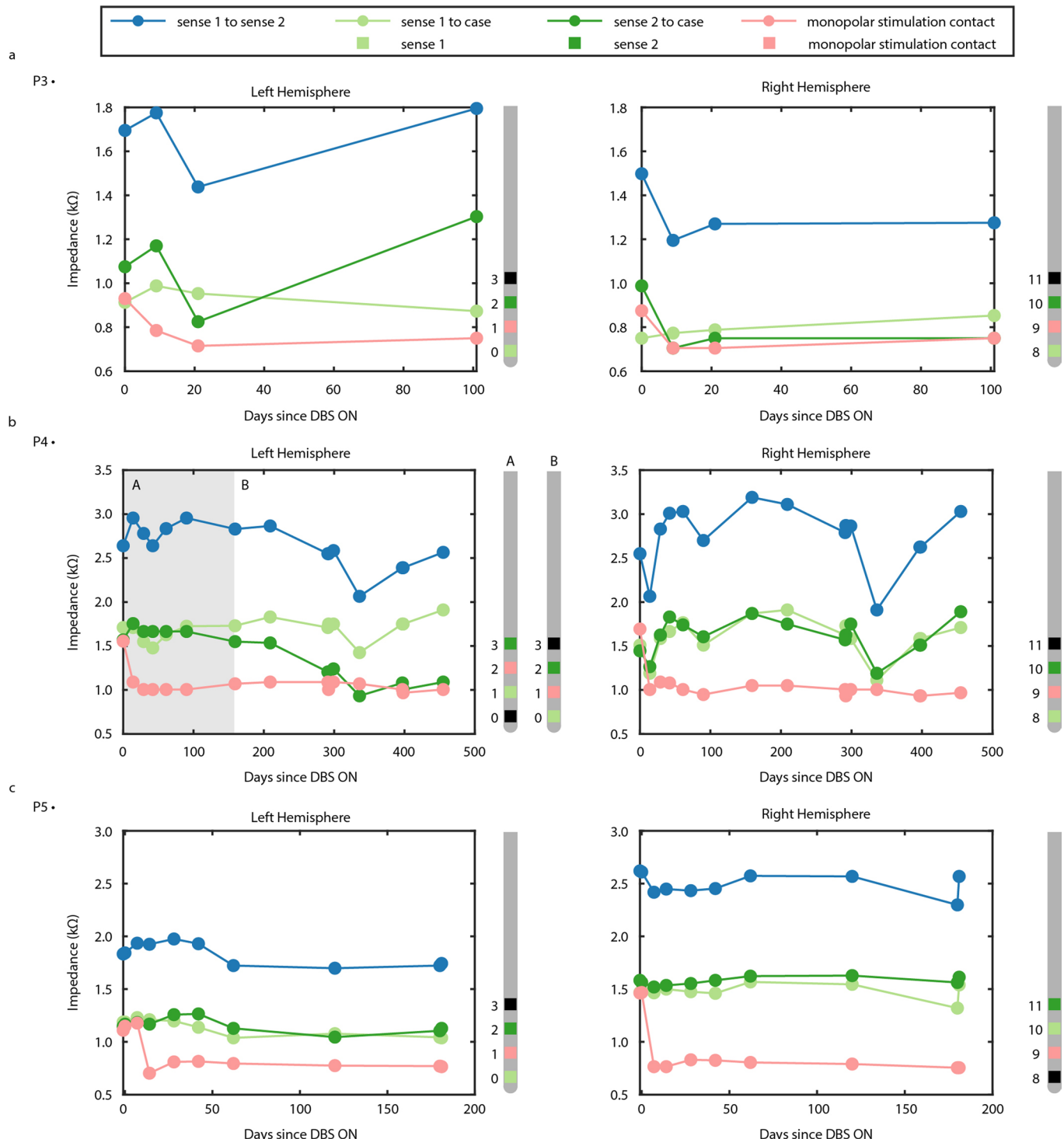
Correspondence and requests for materials should be addressed to David A. Borton.

Peer review information *Nature Medicine* thanks Nolan Williams and the other, anonymous, reviewer(s) for their contribution to the peer review of this work. Jerome Staal was the primary editor on this article and managed its editorial process and peer review in collaboration with the rest of the editorial team.

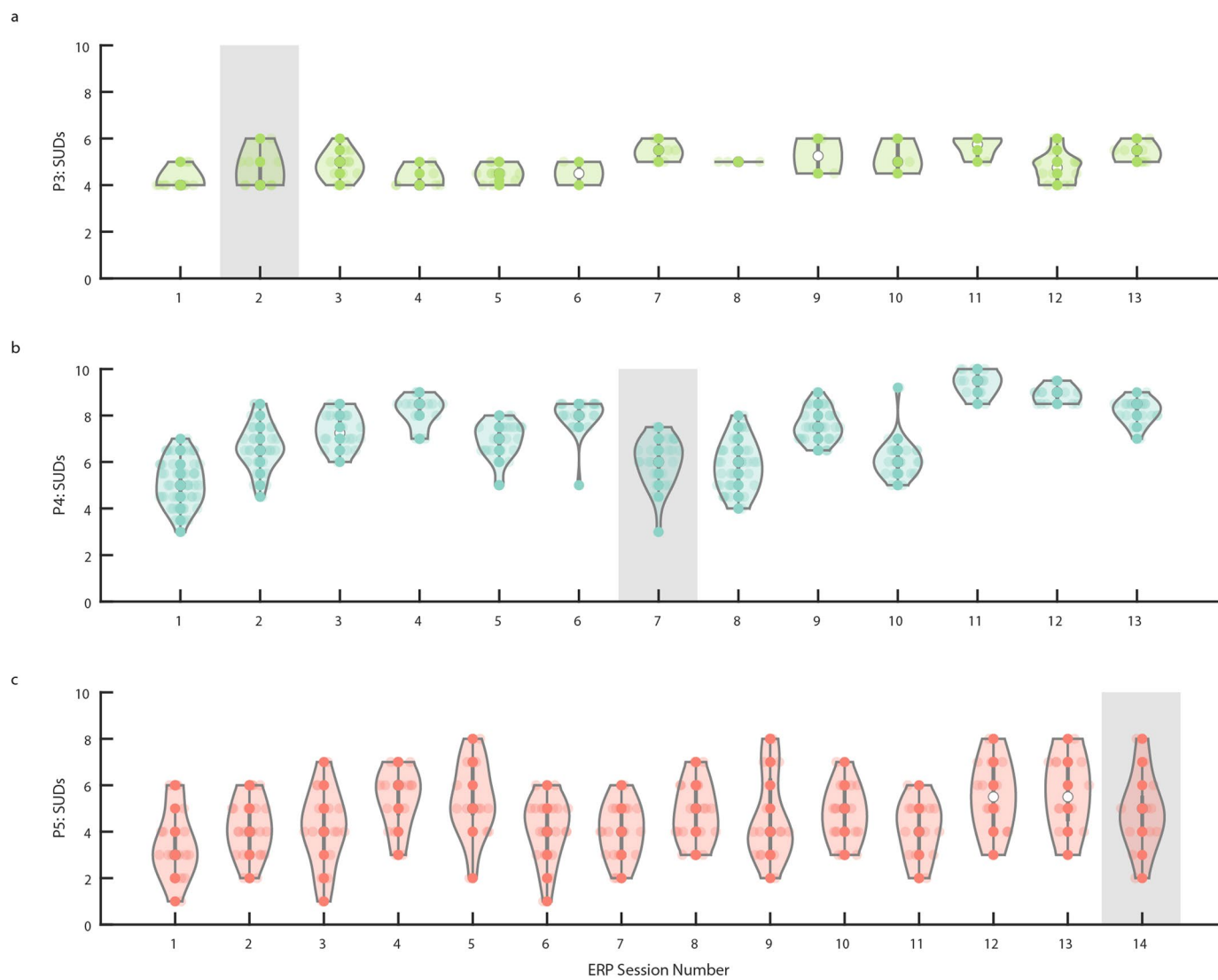
Reprints and permissions information is available at www.nature.com/reprints.



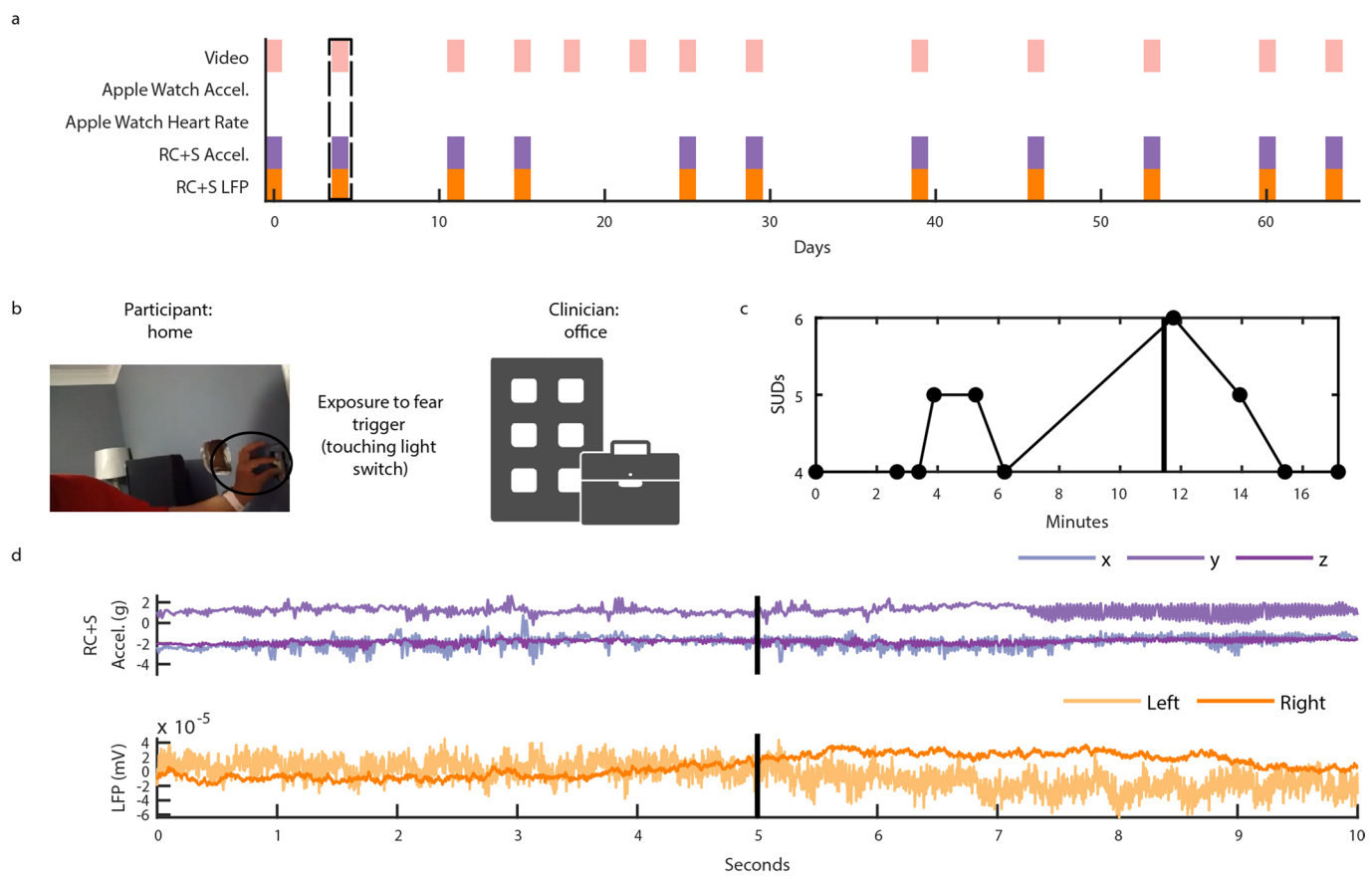
Extended Data Fig. 1 | Anatomical localization of DBS lead placement (P1, P2, P3, P5). (a, b) Coronal (a) and axial (b) T1-weighted (T1w) MRI in radiographic convention from participants P1, P2, P3, and P5 overlaid with reconstructed DBS lead trajectories. Colored regions indicate anterior commissure (AC), caudate, putamen, and ventral striatum (VS). The MRI slice shown is immediately posterior (a; coronal) or inferior (b; axial) to the most ventral contact. Enlarged coronal slices (corresponding to white box outlines in panel a) showing DBS contact locations in each hemisphere are shown on either side of the full coronal slice. Green spheres indicate sensing contacts, red spheres indicate stimulating contacts, black spheres indicate contacts that were used for neither stimulation nor sensing. In each participant, the tips of the leads were targeted to either the VS or the bed nucleus of the stria terminalis (BNST) (target regions for each participant are included in Extended Data Table 1). Enlarged slices shown are immediately posterior to the most ventral contact in each hemisphere. Anterior-posterior slice location (y) is referenced to the posterior border of the AC, which is defined as $y=0$. (d, e) Front (d) and top-down (e) view of the reconstructed cortical surface, subcortical structures, DBS leads, and AC, shown in radiographic convention.



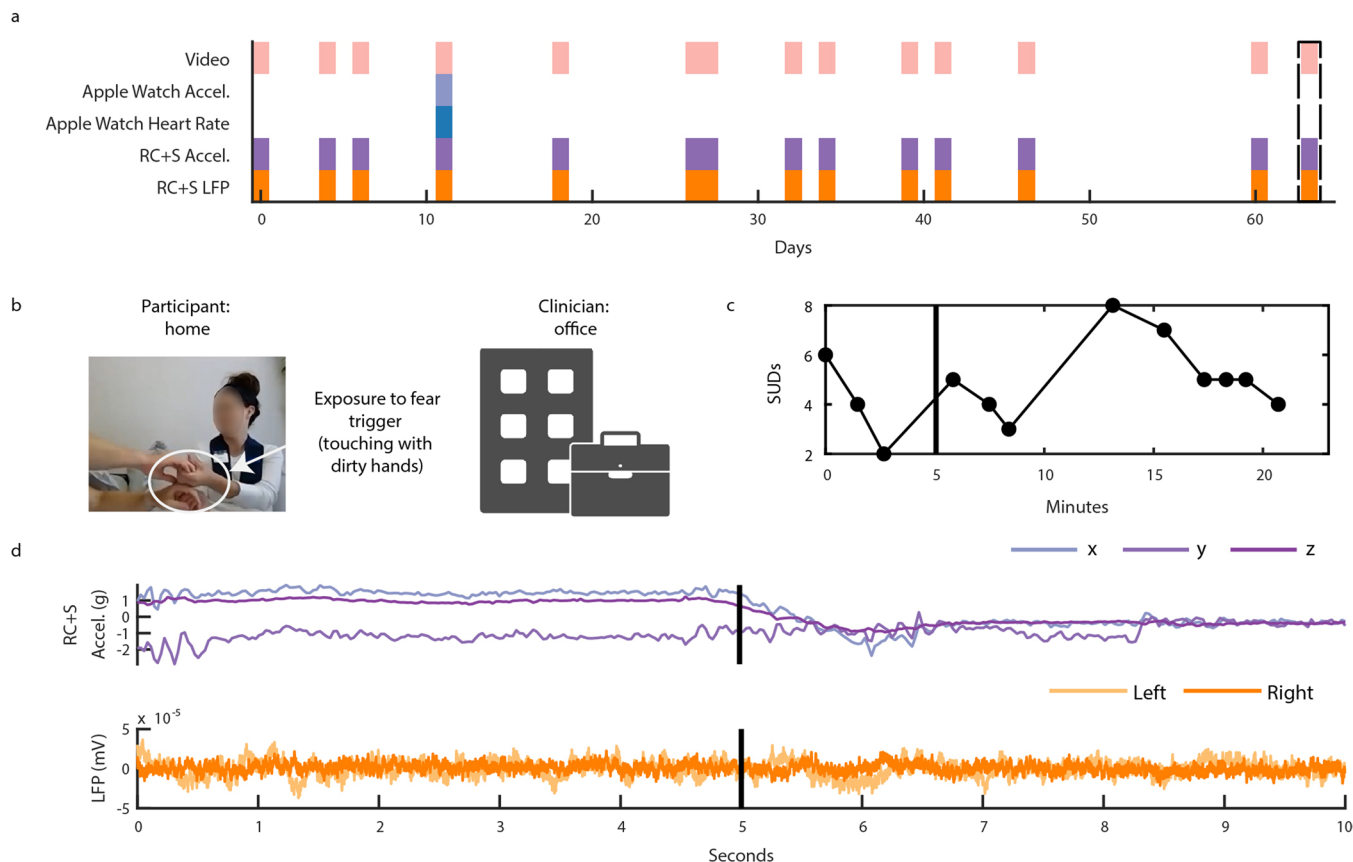
Extended Data Fig. 2 | Impedance of sensing and stimulation electrode contacts reflect long term stability at device-tissue interface. (a) Impedance in kOhms of sensing and stimulation electrode contacts in the left (left panel) and right (right panel) VC/VS of P3. Blue points indicate impedance between the two sensing contacts. Green points indicate the impedance between the deepest (light green) and shallowest (dark green) sensing contact and the INS case. Light red points indicate the impedance between the stimulation contact and the INS case. Sense and stimulation electrode contacts on the Medtronic 3387 leads are visualized to the right of each panel, with contact 0 as the deepest contact on the left, and contact 8 as the deepest contact on the right. Light green indicates the deepest sensing contact, Green indicates the shallowest sensing contact, and light red indicates the stimulation contact. Black contacts are unused. (b) Impedance in kOhms of sensing and stimulation electrode contacts in the left (left panel) and right (right panel) VC/VS of P4. Gray shaded region indicates the timespan when sensing and stimulation contacts correspond to the Medtronic 3387 lead diagram labelled with "A", whereas the following timespan with no shading corresponds to the Medtronic 3387 lead diagram labelled with "B". Otherwise, the format is identical to panel a. (c) Impedance in kOhms of sensing and stimulation electrode contacts in the left (left panel) and right (right panel) VC/VS of P5. Format is identical to panel A.



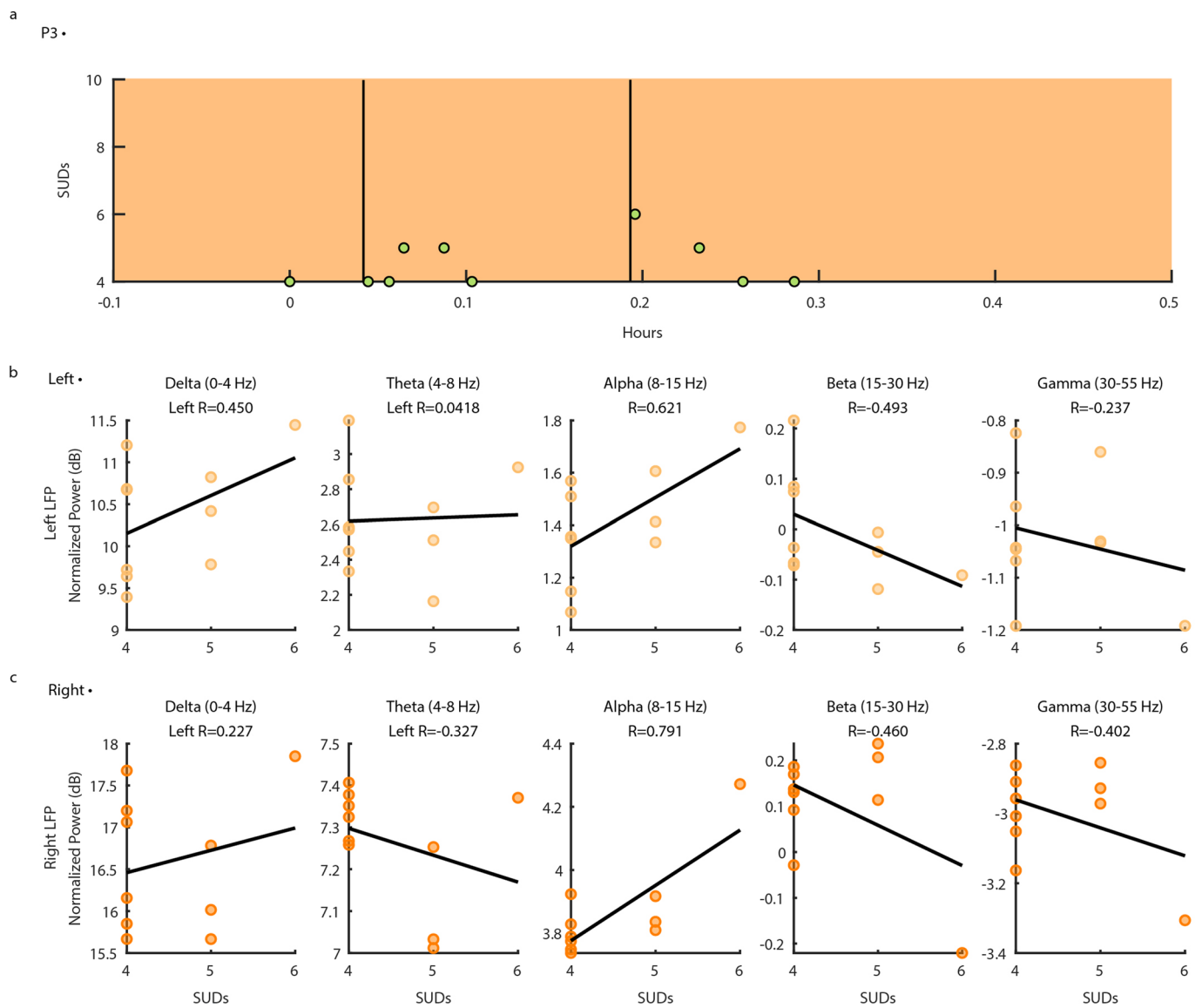
Extended Data Fig. 3 | Distribution of self-reported, Subjective Units of Distress (SUDs) ratings collected by participants during Exposure Response Prevention (ERP) teletherapy. (a) The distribution of SUDs ratings by participant P3 for all recorded sessions. The Y-axis shows SUDs ratings provided by the participant after being prompted to indicate their level of OCD related distress at irregular time intervals during each ERP session on a scale of 0–10 with 0 representing ‘no distress’ and 10 representing ‘the worst distress.’ The X-Axis shows each consecutive, hour-long, recorded ERP session ($n=13$ to $n=14$ for each participant) completed. Gray shading indicates the session analyzed in Extended Data Fig. 6. (b) The distribution of SUDs ratings by participant P4 for all recorded sessions. Format is identical to panel A. Gray shading indicates the session analyzed in Extended Data Fig. 7. (c) The distribution of SUDs ratings by participant P5 for all recorded sessions. Format is identical to panel A. Gray shading indicates the session analyzed in Extended Data Fig. 8.



Extended Data Fig. 4 | Intracranial electrophysiology during Exposure and Response Prevention (ERP) teletherapy at home with Participant P3. (a) Calendar availability plot of ERP sessions for participant P4, over days since the first ERP session. Shaded portions indicate data availability for ERP video, Apple watch heart rate, Apple watch acceleration, RC + S acceleration, and RC + S LFP. Rectangular dotted line corresponds to the ERP session example data shown in panels B-D. (b) Video of participant P4 (left), clinician (right). (c) Time-course in minutes of self-reported Subjective Units of Distress (SUDs) ratings. Vertical black line corresponds to the video frame shown in panel b. (d) Ten seconds of example data synchronized to video, including RC + S acceleration, and two bipolar LFP channels. Vertical black line corresponds to the video frame shown in panel B.

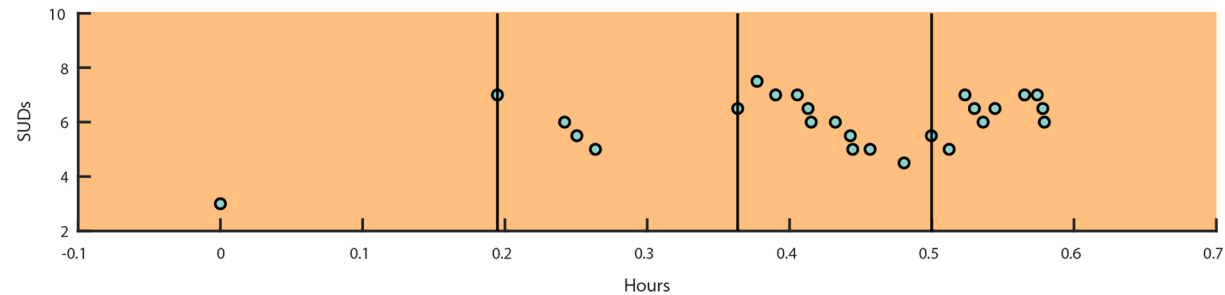


Extended Data Fig. 5 | Intracranial electrophysiology during Exposure and Response Prevention (ERP) teletherapy at home with Participant P5. (a) Calendar availability plot of ERP sessions for participant P4, over days since the first ERP session. Shaded portions indicate data availability for ERP video, Apple watch heart rate, Apple watch acceleration, RC + S acceleration, and RC + S LFP. Rectangular dotted line corresponds to the ERP session example data shown in panels b-d. (b) Video of participant P4 (left), clinician (right). (c) Time-course in minutes of self-reported Subjective Units of Distress (SUDs) ratings. Vertical black line corresponds to the video frame shown in panel b. (d) Ten seconds of example data synchronized to video, including RC + S acceleration, and two bipolar LFP channels. Vertical black line corresponds to the video frame shown in panel b.

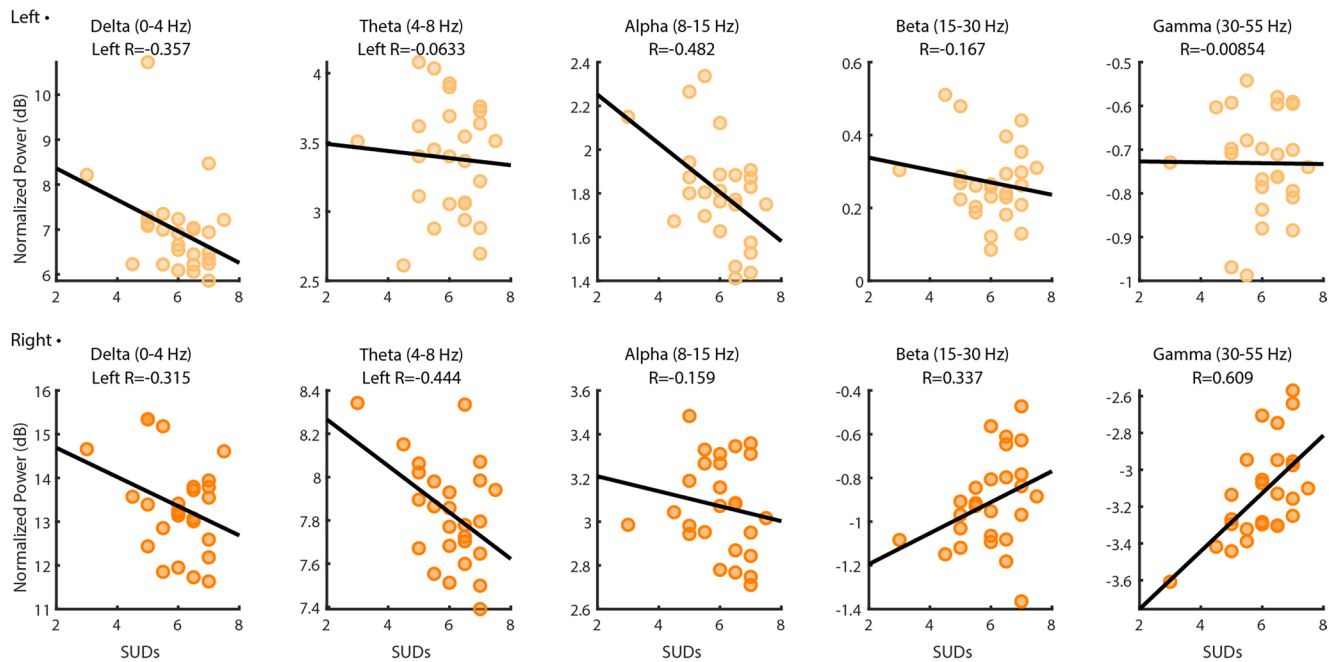


Extended Data Fig. 6 | Ventral Capsule/Ventral Striatum spectral activity vs. SUDs ratings during P3 Exposure and Response Prevention (ERP)

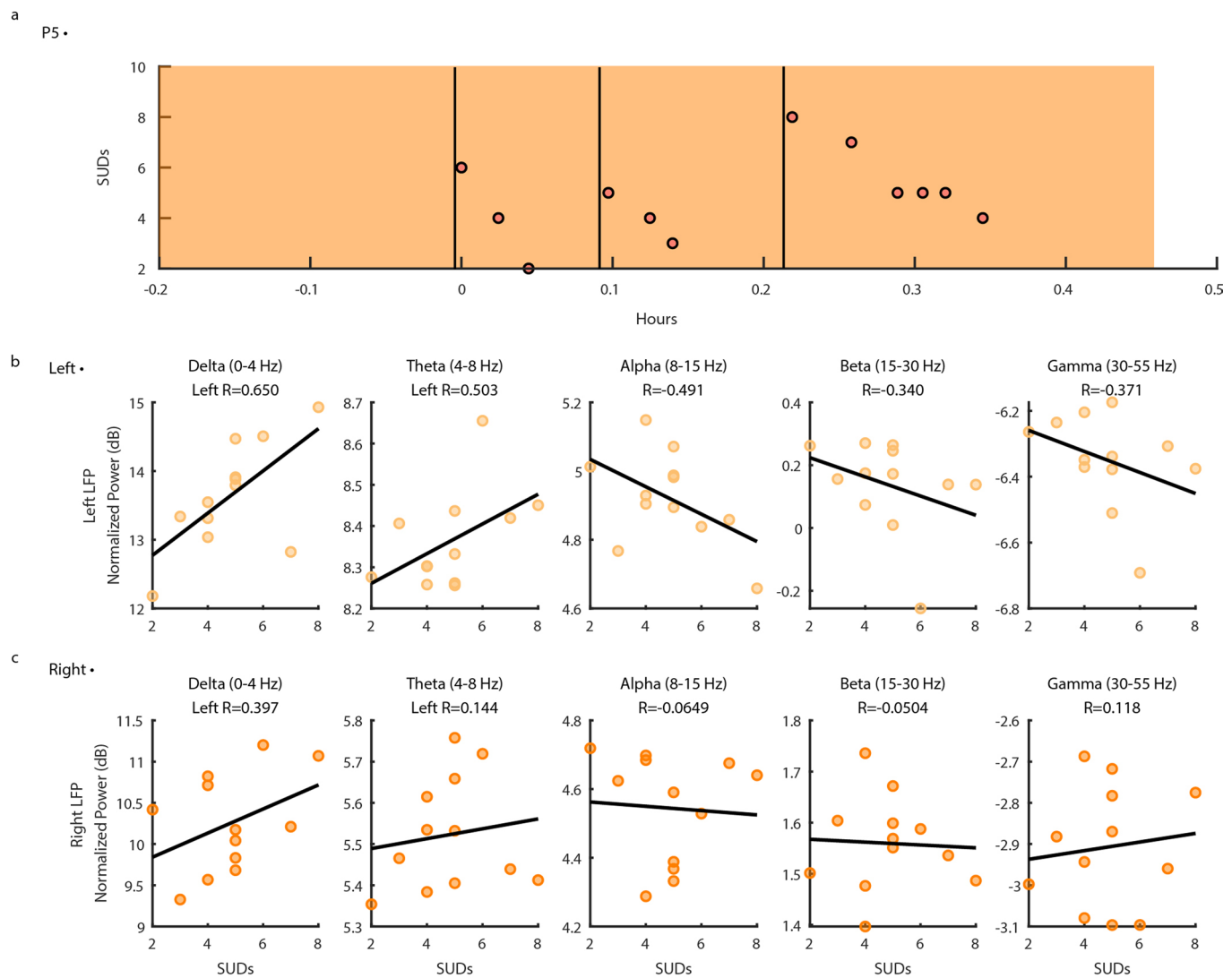
teletherapy recording. (a) Self-reported intensity of OCD symptoms (scatter points) shown over time in hours with LFP data availability (orange shading). Vertical black lines indicate timepoints of OCD exposures. (b) Normalized left VC/VS spectral power in Delta (0-4 Hz), Theta (4-8 Hz), Alpha (8-15 Hz), Beta (15-30 Hz), and Gamma (30-55 Hz) (from left to right) vs. self-reported OCD symptom intensity from zero to 10. Black lines represent the line of least squares. R values correspond to the coefficient of correlation. (c) Normalized right VC/VS spectral power in frequency bands of interest vs. self-reported OCD symptom intensity from zero to 10. Format is identical to panel b.

a
P4 •

b

**Extended Data Fig. 7 | Ventral Capsule/Ventral Striatum spectral activity vs. SUDs ratings during P4 Exposure and Response Prevention teletherapy**

recording. (a) Self-reported intensity of OCD symptoms (scatter points) shown over time in hours with LFP data availability (orange shading). Vertical black lines indicate timepoints of OCD exposures. (b) Normalized left VC/VS spectral power in Delta (0-4 Hz), Theta (4-8 Hz), Alpha (8-15 Hz), Beta (15-30 Hz), and Gamma (30-55 Hz) (from left to right) vs. self-reported OCD symptom intensity from zero to 10. Black lines represent the line of least squares. R values correspond to the coefficient of correlation. (c) Normalized right VC/VS spectral power in frequency bands of interest vs. self-reported OCD symptom intensity from zero to 10. Format is identical to panel B.



Extended Data Fig. 8 | Ventral Capsule/Ventral Striatum spectral activity vs. SUDs ratings during P5 Exposure and Response Prevention teletherapy recording. **(a)** Self-reported intensity of OCD symptoms (scatter points) shown over time in hours with LFP data availability (orange shading). Vertical black lines indicate timepoints of OCD exposures. **(b)** Normalized left VC/VS spectral power in Delta (0-4 Hz), Theta (4-8 Hz), Alpha (8-15 Hz), Beta (15-30 Hz), and Gamma (30-55 Hz) (from left to right) vs. self-reported OCD symptom intensity from zero to 10. Black lines represent the line of least squares. R values correspond to the coefficient of correlation. **(c)** Normalized right VC/VS spectral power in frequency bands of interest vs. self-reported OCD symptom intensity from zero to 10. Format is identical to panel **b**.

Extended Data Table 1 | Participant demographics, DBS surgery device and targets, and stimulation and sensing contact information

Participant:	P1	P2	P3	P4	P5
Gender	Male	Female	Female	Male	Female
Age at time of consent	31	39	37	40	31
Race	White	White	White	White	White
Ethnicity	Not Hispanic/Latino	Hispanic/Latino	Hispanic/Latino	Not Hispanic/Latino	Not Hispanic/Latino
Primary diagnosis	OCD	OCD	OCD	OCD	OCD
Comorbid diagnoses	MDD	PTSD, MDD, GAD	PTSD, MDD, TS	Bipolar Disorder II	MDD
Principal OCD symptoms	Intrusive aggressive/taboo obsessions with checking and repeating rituals	Intrusive aggressive/sexual taboo obsessions with checking and repeating rituals	Intrusive aggressive thoughts, magical thinking, and scrupulosity with checking and repeating rituals	Contamination and scrupulosity obsessions with cleaning and checking rituals	Intrusive aggressive and contamination obsessions with checking and cleaning rituals
Age of OCD onset (years)	17	18	12	16	8
Responder status	Yes	Yes	Yes	Yes	Yes
Initial Y-BOCS II (Y-BOCS) score	37 (35)	39 (34)	46 (40)	42 (38)	47 (37)
Final Y-BOCS II (Y-BOCS) score	8 (6)	11 (9)	27 (25)	25 (22)	26 (23)
DBS Device	PC+S	PC+S	RC+S	RC+S	RC+S
DBS Target Region	L BNST R BNST	BNST BNST	VCVS VCVS	VCVS BNST	BNST BNST
Stimulating Contact	L 1-/C+ R 10-/C+	2-/C+ OFF	1-/C+ 9-/C+	1-/C+ 9-/C+	1-/C+ 9-/C+
Sensing contact	L 0-2 R 9-11	1-3 9-11	0-2 8-10	0-2 8-10	0-2 10-11
Final DBS Rate	L 150 Hz R 150 Hz	150 Hz OFF	150.6 Hz 150.6 Hz	150.6 Hz 150.6 Hz	150.6 Hz 150.6 Hz
Final DBS Amplitude	L 5.0 V R 5.0 V	5.5 V OFF	6.0 mA 5.7 mA	5.2 mA 5.0 mA	6.0 mA 6.0 mA
Final DBS Pulse Width	L 120 µs R 120 µs	120 µs OFF	210 µs 210 µs	120 µs 120 µs	180 µs 180 µs

MDD: Major Depressive Disorder, PTSD: Post-Traumatic Stress Disorder, GAD: General Anxiety Disorder, TS: Tourette's Syndrome., ET: Essential Tremor. *Responder = 35% or greater decrease in the Yale-Brown Obsessive-Compulsive Scale (Y-BOCS) after 12 months of activation compared to presurgical baseline. N/A refers to participants that have not completed study yet.

Reporting Summary

Nature Research wishes to improve the reproducibility of the work that we publish. This form provides structure for consistency and transparency in reporting. For further information on Nature Research policies, see our [Editorial Policies](#) and the [Editorial Policy Checklist](#).

Statistics

For all statistical analyses, confirm that the following items are present in the figure legend, table legend, main text, or Methods section.

n/a Confirmed

- The exact sample size (n) for each experimental group/condition, given as a discrete number and unit of measurement
- A statement on whether measurements were taken from distinct samples or whether the same sample was measured repeatedly
- The statistical test(s) used AND whether they are one- or two-sided
Only common tests should be described solely by name; describe more complex techniques in the Methods section.
- A description of all covariates tested
- A description of any assumptions or corrections, such as tests of normality and adjustment for multiple comparisons
- A full description of the statistical parameters including central tendency (e.g. means) or other basic estimates (e.g. regression coefficient) AND variation (e.g. standard deviation) or associated estimates of uncertainty (e.g. confidence intervals)
- For null hypothesis testing, the test statistic (e.g. F , t , r) with confidence intervals, effect sizes, degrees of freedom and P value noted
Give P values as exact values whenever suitable.
- For Bayesian analysis, information on the choice of priors and Markov chain Monte Carlo settings
- For hierarchical and complex designs, identification of the appropriate level for tests and full reporting of outcomes
- Estimates of effect sizes (e.g. Cohen's d , Pearson's r), indicating how they were calculated

Our web collection on [statistics for biologists](#) contains articles on many of the points above.

Software and code

Policy information about [availability of computer code](#)

Data collection

Summit RC+S® (Medtronic, Minneapolis, MN, USA) recordings during DBS programming sessions in the clinic were conducted using a clinician-facing application that communicates with the Medtronic Summit Application Programming Interface (API) running on a Surface Pro tablet (<https://github.com/openmind-consortium/App-aDBS-ResearchFacingApp>). At home, participants started their own recording sessions using a patient-facing application (frontend: <https://github.com/openmind-consortium/App-OCD-PatientFrontend>, backend: <https://github.com/openmind-consortium/App-OCD-PatientBackend>) that communicates with the Medtronic Summit API. Participants used the Rune Labs StriveStudy mobile application (Rune Labs Inc., San Francisco, CA) to report their OCD symptom intensity. Behavioral tasks were all developed using Honeycomb, a template for reproducible behavioral tasks for clinic, laboratory, and home use (<https://github.com/brown-ccv/honeycomb>). Data from the Summit RC+S® patient-facing application and behavioral task data was automatically uploaded to Box.com from SurfaceGo tablets via a .BAT script triggered by Windows Task Scheduler upon connecting to the internet, or user login/logout (<https://github.com/neuromotion/rfps-box-upload>).

Data analysis

MATLAB 2018b (Mathworks, Natick, MA, USA) was used for all neural time series data and Automatic Facial Affect Recognition (AFAR) analysis described in the manuscript. Packet loss handling procedures were implemented using code available at <https://github.com/openmind-consortium/Analysis-rcs-data>. An automatic cortical reconstruction was performed on the preoperative T1w MRI using FreeSurfer v6.0 (<http://surfer.nmr.mgh.harvard.edu>). The postoperative CT was aligned to the preoperative T1w MRI using the Functional Magnetic Resonance Imaging for the Brain Software Library's (FMRIB's) Linear Image Registration Tool v6.0 (FLIRT: <https://fsl.fmrib.ox.ac.uk/fsl/fslwiki/FLIRT>). Electrode coordinates were manually determined from the co-registered CT in BiolImage Suite v3.5b1 (<https://bioimagesuiteweb.github.io/webapp/>). The reconstructed cortical surface (pial surface), segmented subcortical structures, and electrode coordinates were visualized using the Multi-Modal Visualization Tool (MMVT; <https://mmvt.mgh.harvard.edu/>).

For manuscripts utilizing custom algorithms or software that are central to the research but not yet described in published literature, software must be made available to editors and reviewers. We strongly encourage code deposition in a community repository (e.g. GitHub). See the Nature Research [guidelines for submitting code & software](#) for further information.

Data

Policy information about [availability of data](#)

All manuscripts must include a [data availability statement](#). This statement should provide the following information, where applicable:

- Accession codes, unique identifiers, or web links for publicly available datasets
- A list of figures that have associated raw data
- A description of any restrictions on data availability

The datasets generated during and/or analyzed during the current study will be publicly available once the study is completed. At the completion of the study, all data will be deposited in the NIH Data Archive for the Brain Initiative®. In the interim, the minimum dataset and code required to recreate figure 4D, figure 6, extended data figures 6-8 is available upon request to the corresponding author.

Field-specific reporting

Please select the one below that is the best fit for your research. If you are not sure, read the appropriate sections before making your selection.

Life sciences Behavioural & social sciences Ecological, evolutionary & environmental sciences

For a reference copy of the document with all sections, see nature.com/documents/nr-reporting-summary-flat.pdf

Life sciences study design

All studies must disclose on these points even when the disclosure is negative.

Sample size	Overall, among all phases of the 5 year study, we expect to enroll 20 DBS subjects to achieve our n=10 implanted subjects. The overall study will include 10 DBS subjects between the ages of 21 and 70 with severe, treatment-resistant OCD. Five DBS subjects will initially be recruited to Phase 1. Upon completion of Phase 1, an additional five subjects will be recruited to Phase 2. This work includes data from the first 5 subjects (N=5) that represent all of the subjects that have been implanted to date.
Data exclusions	No data relevant to this report was excluded. Where indicated in the main text, example data is shown to illustrate proof-of-concept.
Replication	This is a N=5 report, and findings should be replicated across a larger population of subjects.
Randomization	The data was not randomized, as this is a proof-of-concept report. Treatment is open label, and subjects serve as their own controls via the blinded discontinuation phase.
Blinding	Blinding occurred during the discontinuation period after 8 months of open label therapy. At the end of month 8 after DBS implant, all subjects entered a one-month delayed onset withdrawal period in which the subject and Independent Evaluators were blinded to timing of discontinuation. In all cases, the sequence was as follows in one-week segments: 100% Active, 50% Active, Sham and Sham. Subjects were seen weekly. Amplitude was reduced by 50% at start of week 2 and turned off at start of week 3. Subjects were told that DBS will be discontinued at some point during the 4 weeks. The purpose of the 50% initial reduction is to minimize rebound effects. The programmer was open to the design and performed "sham" activation.

Reporting for specific materials, systems and methods

We require information from authors about some types of materials, experimental systems and methods used in many studies. Here, indicate whether each material, system or method listed is relevant to your study. If you are not sure if a list item applies to your research, read the appropriate section before selecting a response.

Materials & experimental systems

n/a	Involved in the study
<input checked="" type="checkbox"/>	<input type="checkbox"/> Antibodies
<input checked="" type="checkbox"/>	<input type="checkbox"/> Eukaryotic cell lines
<input checked="" type="checkbox"/>	<input type="checkbox"/> Palaeontology and archaeology
<input checked="" type="checkbox"/>	<input type="checkbox"/> Animals and other organisms
<input type="checkbox"/>	<input checked="" type="checkbox"/> Human research participants
<input type="checkbox"/>	<input checked="" type="checkbox"/> Clinical data
<input checked="" type="checkbox"/>	<input type="checkbox"/> Dual use research of concern

Methods

n/a	Involved in the study
<input checked="" type="checkbox"/>	<input type="checkbox"/> ChIP-seq
<input checked="" type="checkbox"/>	<input type="checkbox"/> Flow cytometry
<input type="checkbox"/>	<input checked="" type="checkbox"/> MRI-based neuroimaging

Human research participants

Policy information about [studies involving human research participants](#)

Population characteristics

Five adult subjects with a principal diagnosis of severe and intractable OCD underwent DBS surgery after being apprised of

Population characteristics

the risks, possible benefits and alternatives to participation in the research study. All subjects had OCD for more than five years and failed, or were unable to tolerate, adequate trials of multiple medications (i.e., selective serotonin reuptake inhibitors (SSRIs), clomipramine, and SSRI plus antipsychotics) and as well as a course of Exposure and Response Prevention (ERP) therapy.

Participant P1: 31 years old at the time of consent, white male, comorbid diagnosis of major depressive disorder
 Participant P2: 39 years old at the time of consent, Hispanic female, comorbid diagnoses of post traumatic stress disorder, major depressive disorder, and generalized anxiety disorder
 Participant P3: 37 years old at the time of consent, Hispanic female, comorbid diagnoses of post traumatic stress disorder, major depressive disorder, and tourette syndrome
 Participant P4: 40 years old at the time of consent, white male, comorbid diagnosis of bipolar disorder II
 Participant P5: 31 years old white female at the time of consent, white female, comorbid diagnosis of major depressive disorder

Recruitment

The primary source of OCD subjects were self-referrals generated through BCM clinical trials website, Clinicaltrials.gov, and BCM Psychiatry Clinic. We also received referrals from area clinicians in addition to BCM affiliates. Potential participants were given the contact information of the PI and research coordinator and/or the participant completed a study contact form so research staff could contact the potential subject directly. In some cases, participants learned of the study through consumer advocacy groups such as the International OCD Foundation (IOCDF), local non-profit organizations and local support group meetings and through the normal avenues that they share information. None of the participants were current or prior patients of the Principal Investigator. While we recognize the many potential incentives for participants to enroll in the study to effectively treat their disease, we don't think there is self selection bias due to the invasive nature and considerable potential risks of DBS surgery.

Ethics oversight

All procedures were approved by the local institutional review board at Baylor College of Medicine (H-40255 and H-44941 to Baylor College of Medicine, IAA 17-27 and IAA 19-51 to Brown University, and STUDY20110082 and STUDY20110084 to University of Pittsburgh) and the US. Food and Drug Administration Center for Devices and Radiological Health. The study was monitored by a Data Safety Monitoring Board (DSMB) that convened quarterly. We also work with a neuroethicist that specializes in ethics of Deep Brain Stimulation.

Note that full information on the approval of the study protocol must also be provided in the manuscript.

Clinical data

Policy information about [clinical studies](#)

All manuscripts should comply with the ICMJE [guidelines for publication of clinical research](#) and a completed [CONSORT checklist](#) must be included with all submissions.

Clinical trial registration

[NCT04281134](#), [NCT03457675](#)

Study protocol

<https://clinicaltrials.gov/ct2/show/NCT04281134>, <https://clinicaltrials.gov/ct2/show/NCT03457675>

Data collection

Data was collected over the course of October 2018 to June 2021 in the clinic at Baylor College of Medicine and in the homes of participants (P3, P4, P5).

Outcomes

Primary Outcome Measures

Percent of subjects that display biomarkers of OCD-related distress (Time Frame: Month 6) electrophysiological signals (deep brain local field potentials with scalp electroencephalography) from the brain showing Cohen's kappa $k > 0.40$, chance corrected classification agreement with OCD-related distress during task exposure in clinic.

Percent of subjects that display biomarkers of OCD-related distress (Time Frame: Month 9) electrophysiological signals (deep brain local field potentials with scalp electroencephalography) from the brain showing Cohen's kappa $k > 0.40$, chance corrected classification agreement with OCD-related distress during task exposure in clinic.

Percent of subjects that display biomarkers of OCD-related distress (Time Frame: Month 12) electrophysiological signals (deep brain local field potentials with scalp electroencephalography) from the brain showing Cohen's kappa $k > 0.40$, chance corrected classification agreement with OCD-related distress during task exposure in clinic.

Percent of subjects that display biomarkers of OCD-related distress (Time Frame: Month 18) electrophysiological signals (deep brain local field potentials with scalp electroencephalography) from the brain showing Cohen's kappa $k > 0.40$, chance corrected classification agreement with OCD-related distress during task exposure in clinic.

Percent of subjects that display biomarkers of DBS-induced hypomania (Time Frame: Month 6) electrophysiological signals (deep brain local field potentials with scalp electroencephalography) from the brain showing Cohen's kappa $k > 0.40$, chance corrected classification agreement with DBS therapy during clinical visits.

Percent of subjects that display biomarkers of DBS-induced hypomania (Time Frame: Month 9) electrophysiological signals (deep brain local field potentials with scalp electroencephalography) from the brain showing Cohen's kappa $k > 0.40$, chance corrected classification agreement with DBS therapy during clinical visits.

Percent of subjects that display biomarkers of DBS-induced hypomania (Time Frame: Month 12) electrophysiological signals (deep brain local field potentials with scalp electroencephalography) from the brain showing Cohen's kappa $k > 0.40$, chance corrected classification agreement with DBS therapy during clinical visits.

Percent of subjects that display biomarkers of DBS-induced hypomania (Time Frame: Month 18)

electrophysiological signals (deep brain local field potentials with scalp electroencephalography) from the brain showing Cohen's kappa $k > 0.40$, chance corrected classification agreement with DBS therapy during clinical visits.

Secondary Outcome Measures

Change in Yale-Brown Obsessive Compulsive Scale (Y-BOCS) Rating OCD Symptom Severity (Time Frame: Baseline to 30 days)
Changes in the Yale-Brown Obsessive Compulsive Scale survey/questionnaire. This is measured after closed-loop stimulation and is an assessment to rate symptoms of OCD on a scale of 0-50 (with a higher number indicating a more severe outcome ratings of OCD and 0 indicated no symptoms of OCD).

Magnetic resonance imaging

Experimental design

Design type	Resting state
Design specifications	N/A
Behavioral performance measures	N/A

Acquisition

Imaging type(s)	Structural
Field strength	1.5T and 3T
Sequence & imaging parameters	High resolution (0.8 mm isotropic) T1-weighted (T1w) anatomical images (MPRAGE; TR/TE/TI=2400/2.24/1000 ms, flip angle=8°, TA ~ 7 min) were acquired. T2-weighted (T2w) images (SPACE; 0.8mm isotropic; TR/TE = 3200/563ms, TA ~6min) were acquired in the same session.
Area of acquisition	Whole brain scan
Diffusion MRI	<input type="checkbox"/> Used <input checked="" type="checkbox"/> Not used

Preprocessing

Preprocessing software	An automatic cortical reconstruction was performed on the preoperative T1w MRI using FreeSurfer v7.1.1 (http://surfer.nmr.mgh.harvard.edu) and the T2w MRI was used to improve reconstruction of the pial surfaces. The postoperative CT was aligned to the preoperative T1w MRI using the Functional Magnetic Resonance Imaging for the Brain Software Library's (FMRIb's) Linear Image Registration Tool v6.0 (FLIRT). Electrode coordinates were manually determined from the co-registered CT in Biolmage Suite v3.5b1 and placed into the native MRI space. The reconstructed cortical surface (pial surface), segmented subcortical structures, and electrode coordinates were visualized using the Multi-Modal Visualization Tool (MMVT). The caudate, putamen, and the ventral striatum were colored on the T1w slice based on the subcortical segmentation. Anterior Commissure (AC) was manually reconstructed by tracing the white fiber tracts on the T1w MRI slice.
Normalization	FreeSurfer v7.1.1 was used to perform intensity normalization (within the 'recon-all' step), during which the signal intensity of the white and gray matter was homogenized in order to better distinguish between the tissue types and more easily segment the brain.
Normalization template	N/A
Noise and artifact removal	N/A
Volume censoring	N/A

Statistical modeling & inference

Model type and settings	N/A
Effect(s) tested	N/A
Specify type of analysis:	<input checked="" type="checkbox"/> Whole brain <input type="checkbox"/> ROI-based <input type="checkbox"/> Both
Statistic type for inference (See Eklund et al. 2016)	N/A
Correction	N/A

Models & analysis

n/a	Involved in the study
<input checked="" type="checkbox"/>	Functional and/or effective connectivity
<input checked="" type="checkbox"/>	Graph analysis
<input checked="" type="checkbox"/>	Multivariate modeling or predictive analysis